Annu. Rev. Astron. Astrophys. 1996. 34:111–54

BIPOLAR MOLECULAR OUTFLOWS FROM YOUNG STARS AND PROTOSTARS

Rafael Bachiller

Observatorio Astronómico Nacional (IGN), Campus Universitario, Apartado 1143, E–28800 Alcalá de Henares (Madrid), Spain

KEY WORDS: star formation, interstellar medium, interstellar molecules, jets

ABSTRACT

A violent outflow of high-velocity gas is one of the first manifestations of the formation of a new star. Such outflows emerge bipolarly from the young object and involve amounts of energy similar to those involved in accretion processes. The youngest (proto-)stellar low-mass objects known to date (the Class 0 protostars) present a particularly efficient outflow activity, indicating that outflow and infall motions happen simultaneously and are closely linked since the very first stages of the star formation processes.

This article reviews the wealth of information being provided by large millimeter-wave telescopes and interferometers on the small-scale structure of molecular outflows, as well as the most recent theories about their origin. The observations of highly collimated CO outflows, extremely high velocity (EHV) flows, and molecular "bullets" are examined in detail, since they provide key information on the origin and propagation of outflows. The peculiar chemistry operating in the associated shocked molecular regions is discussed, highlighting the recent high-sensitivity observations of low-luminosity sources. The classification schemes and the properties of the driving sources of bipolar outflows are summarized with special attention devoted to the recently identified Class 0 protostars. All these issues are crucial for building a unified theory on the mass-loss phenomena in young stars.

0066-4146/96/0915-0111$08.00

1. INTRODUCTION

The study of mass-loss phenomena from young stars started in the early 1950s with the discovery by Herbig (1951) and Haro (1952) of small nebulosities with peculiar emission line spectra. The so-called Herbig-Haro (HH) objects were soon associated with stellar winds (Osterbrock 1958) and later found to be due to the interaction of a highly supersonic stellar wind with the ambient surrounding material (Schwartz 1975). Measurements of proper motions (Cudworth & Herbig 1979) confirmed that the ejection originates from a newly formed star. Moreover, the rapidly moving highly collimated HH jets, discovered in the visible by Mundt & Fried (1983), also originate from young star positions. On the other hand, the presence of winds around young T Tauri stars was recognized in their P Cygni profiles (Herbig 1962, Kuhi 1964) and in centimeter wavelength continuum observations (Cohen et al 1982).

Broad lines of CO at millimeter wavelengths generated by high-velocity molecular gas were discovered toward the Orion A molecular cloud in the mid-1970s (Kwan & Scoville 1976, Zuckerman et al 1976). High-velocity CO emission was soon detected toward other objects, and the structure of the outflowing material was found to be bipolar (Snell et al 1980, Rodríguez et al 1980). The first surveys revealed that these bipolar outflows are extraordinarily common around young stars (Bally & Lada 1983; Edwards & Snell 1982, 1983, 1984). Lada (1985) compiled the first catalog, which contained 68 outflow sources. Further searches carried out with unbiased selection criteria by using, for example, the *IRAS* data base, or the systematic observation of a full molecular cloud in CO lines, led to the detection of many more outflows. Fukui et al (1993) listed 157 outflows confirmed through complete or partial mapping. Observations since then have increased the number of presently known molecular outflows to nearly 200.

Outflows from young stars are a ubiquitous and energetic phenomenon; they have spectacular observational manifestations over a wide range of wavelengths from the ultraviolet to the radio. In general terms, we are now confident that virtually all young stellar objects (YSOs) undergo periods of copious mass loss. The highest resolution observations available show that the flows emerge bipolarly from a stellar or circumstellar region. The fast well-collimated stellar wind sweeps up the ambient molecular gas in its vicinity, forming two cavities oriented in opposite directions with respect to the central star. The molecular gas displaced from the cavities expands in the form of irregular lobes and incomplete shells and constitutes the CO outflow. However, even the most basic questions about the outflow phenomenon are still a matter of debate. It is not clear yet what physical mechanism produces the outflows, and the underlying stellar or protostellar wind that should sweep up the fast moving molecular gas is proving to be extremely hard to detect.

The new generation of large radiotelescopes and interferometers working at millimeter and submillimeter wavelengths is providing a wealth of information on the small-scale structure of bipolar molecular outflows. In addition to the classical outflows at standard high velocities (SHV, i.e. velocities ranging from a few kilometers per second to about 20 km s^{-1}) whose properties were summarized in the excellent review of Lada (1985), weak CO components that have extremely high velocities (EHV) have been discovered and mapped toward some outflows (e.g. Figure 1). The EHV CO components are reminiscent of the HH jets observed in the visible and seem to be of a different nature than the SHV components (Bachiller & Gómez-González 1992).

The purpose of this article is to review the progress in outflow research since Lada's (1985) review, by taking into account the observations carried out during this ten-year period with millimeter telescopes of high resolution and sensitivity. Special attention is devoted to the extraordinary outflow activity of "Class 0" sources, possibly the youngest (proto-)stellar low-mass objects known to date. Recent theoretical models for the origin of flows and for the interaction of the winds with the molecular surrounding medium are also discussed. Other recent review papers on closely related issues include those by Lada (1991), Bachiller & Gómez-González (1992), Fukui et al (1993), Königl & Ruden (1993), Sargent & Welch (1993), Edwards et al (1993), Cabrit (1993), and Reipurth & Bachiller (1995).

2. THE DIFFERENT COMPONENTS OF BIPOLAR OUTFLOWS

Bipolar outflows from YSOs contain ionized, atomic, and molecular gas in a wide range of excitation conditions. We next describe each of these components in turn and discuss their close relationship. We start by briefly summarizing the properties of the relatively cold molecular gas traced by the classical (SHV) CO outflows. (For a more complete description of their characteristics, see Lada 1985.) This SHV component is usually the most massive, since it consists of a large amount of ambient material that has been swept up during the full period of mass-loss. In contrast, the EHV CO component found in some outflows has different characteristics, and it is separately discussed in Section 3.

2.1 *Molecular Component: Standard CO Outflows*

Molecular outflows with standard high velocities have been extensively studied during the past 15 years (e.g. Bally & Lada 1983; Edwards & Snell 1982, 1983, 1984; Snell et al 1984; Goldsmith et al 1984; Parker et al 1991). Following a first suggestion of Snell et al (1980), there is a wide consensus now that these outflows consist of ambient gas swept up by an underlying wind. These SHV outflows are observed around young stellar objects of very different masses and

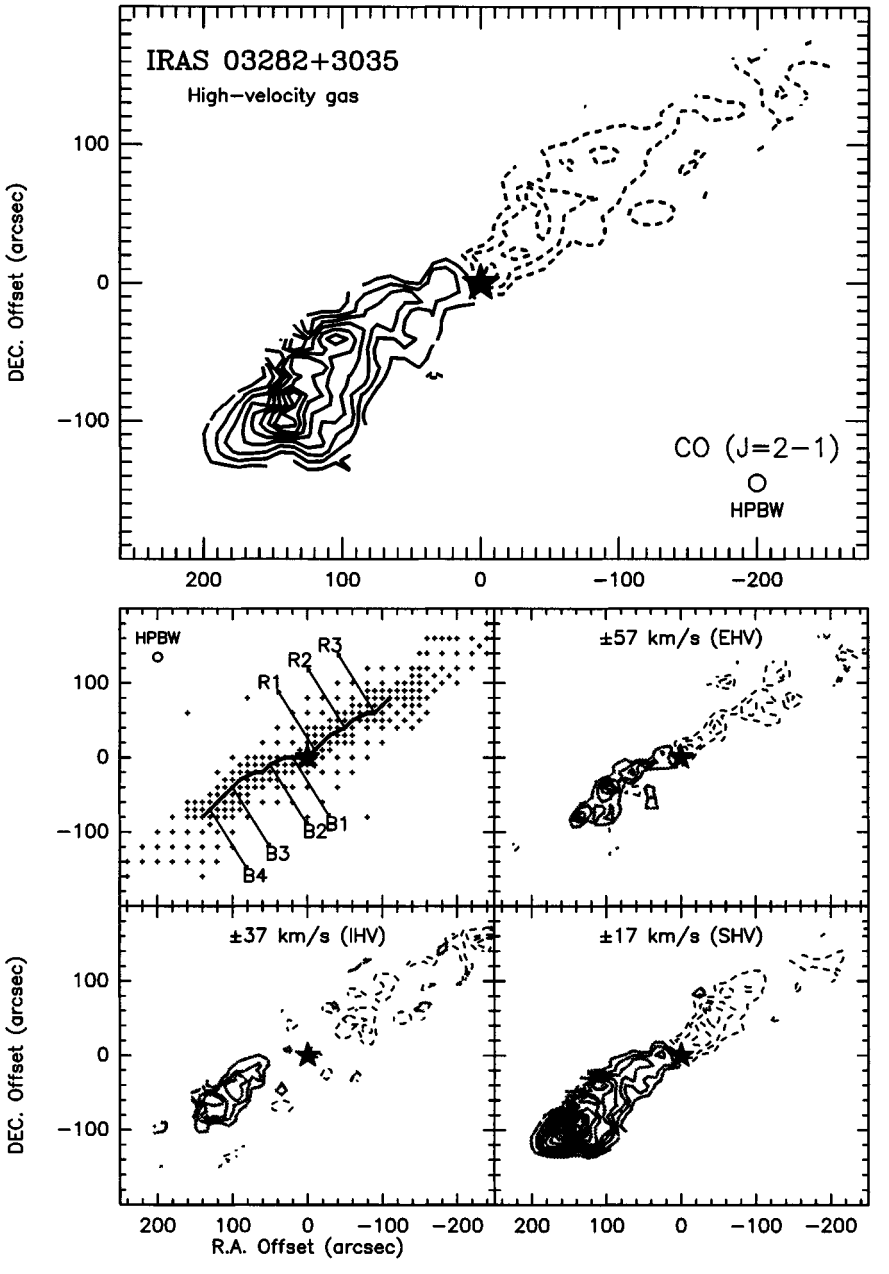

luminosities, with low collimation factors (i.e. the ratio of the outflow length to its width) in the range of 2 to 5.

Most molecular outflows are bipolar, though some monopolar outflows are also reported in the literature (e.g. MWC1080, Bally & Lada 1983). In addition, there is an increasing number of multipolar outflows (e.g.: VLA 16293, Walker et al 1988; 723, Avery et al 1990; HH 111, Cernicharo et al 1996) that could result from the superposition of distinct bipolar outflows. In fact, the widely observed multiplicity of young stars (Mathieu 1994) seems to result in a correspondingly high number of multipolar molecular outflows.

The usual procedures used to estimate the physical parameters of bipolar outflows from CO observations have been summarized by Bachiller & Gómez-González (1992). Estimating the CO optical depth and excitation temperature requires the observation of at least two rotational lines of CO and one line of ^{13}CO. From this, it is then possible to estimate the mass of the outflowing gas (by assuming a CO/H_2 ratio). Estimates of the flow momentum and energy depend critically on knowledge of the inclination of the flow axis to the line of sight, and these can be subject to serious uncertainties (Margulis & Lada 1985, Cabrit & Bertout 1990). Some attempts have been made to model the 3-D kinematic structure of bipolar outflows (Cabrit & Bertout 1986, 1990; Cabrit et al 1988), and the kinematic structure of some particular outflows has been successfully accounted for (RNO43 and B335, Cabrit et al 1988; MonR2, Meyers-Rice & Lada 1991).

The amount of mass in a given molecular flow can range from less than $10^{-2}\ M_\odot$ (e.g. HH 34; Chernin & Masson 1995a, Terebey et al 1989) to about 200 $M_\odot$ (e.g. Mon R2, Wolf et al 1990; DR21, Russell et al 1992). The flow sizes go from less than 0.1 pc (e.g. Ori-I-2, Cernicharo et al 1992) to about 5 pc. The energy deposited in the CO outflow can reach 10^{47}–10^{48} erg (e.g.

←

Figure 1 (*Top*) Map of CO 2–1 intensity integrated in the line wings from the IRAS 03282+3035 outflow. Solid contours represent the blueshifted emission (from −60 km s^{-1} to 0 km s^{-1}), while dashed contours are for the redshifted emission (integrated from 14 km s^{-1} to 74 km s^{-1}). First contour and contour interval are 6 K km s^{-1}. (*Lower panels*) Maps of CO 2–1 line intensity integrated in different velocity intervals. The different panels are for the blueshifted (*solid contours*) and redshifted (*dashed*) emission in a velocity interval of 20 km s^{-1}centered at a velocity offset of ± 57 (*upper right panel*), ± 37 (*lower left*), and ± 17 km s^{-1} (*lower right*), with respect to the ambient cloud velocity, 7 km s^{-1}. In the two maps corresponding to the highest velocity emission, the first contour and the contour interval are 2 and 1 K km s^{-1}, respectively. In the map of lower velocity emission, the first contour and the contour interval are 4 K km s^{-1}. The positions of some high-velocity molecular bullets are indicated on the solid line in the upper left panel. (Adapted from Bachiller et al 1991c.)

DR21, Garden et al 1991). The measured kinematic time scales range from 10^3 to a few 10^5 years.

Clumping is a common characteristic of molecular outflows. From multiline observations of CO, Plambeck et al (1983) derived typical values of the filling factor of 0.1–0.2 in several outflows. Snell et al (1984) found that the filling factor approaches unity at the lowest outflow velocities. Clumps are directly observed in some nearby massive outflows as spatially localized velocity components superimposed to the SHV wings. Multiline CS observations have been used to derive the physical properties of such clumps in NGC 2071 (Kitamura et al 1990) and in Mon R2 (Tafalla et al 1994). In Mon R2, the observed SHV clumps are as dense as the ambient cloud (density of a few 10^5 cm^{-3}), and they have masses of up to several $M_\odot$. Most of the SHV outflowing gas could be in the form of clumps of a wide range of size and mass. The decrease of the filling factor at progressively high velocities seems to indicate that the smaller clumps move faster than the larger ones.

Outflow activity can vary over a wide range of time scales. The case of the L1551 outflow is particularly interesting because this is considered the CO outflow prototype. Recent observations of CO with high angular resolution have revealed that the outflow has passed through at least four periods of copious mass-loss (Figure 2; Bachiller et al 1994a). The duration of each mass-loss epoch and the time elapsed between two of them are both about a few 10^4 years. The mass of molecular material associated with each eruptive event ranges from a few tenths to 1 $M_\odot$. Other signs of variability in L1551 are observed in the visible (Neckel & Staude 1987, Campbell et al 1988, Davis et al 1995), and IRS5—the star driving the outflow—is probably a FU Ori star (Mundt et al 1985, Carr et al 1987). However, the time scales involved in the optical variability are of the order of 10^2–10^3 yr, much shorter than the time scales involved in the CO periodicity.

2.2 *Ionized Component: HH Objects and Radio Jets*

In addition to the molecular emission, bipolar outflows from young stars are also observed in the form of optical and centimeter-wavelength jets of ionized material. Particularly relevant are the optical HH jets (Mundt & Fried 1983, Dopita et al 1982, Mundt et al 1987, Reipurth 1991) observed to emerge from a wide variety of YSOs. One of the best examples is the HH 34 system, which contains multiple bow shocks (Reipurth et al 1986, Bührke et al 1988, Reipurth & Heathcote 1992, Morse et al 1992) and extends up to 1.5 pc (Bally & Devine 1994). Many HH jets have associated CO outflows, and in such cases the HH jet and the corresponding CO outflow have the same orientation, similar extension, and compatible kinematics. This is the case for HH 34 (Chernin & Masson 1995a), HH 111 (Reipurth & Cernicharo 1995, Cernicharo & Reipurth

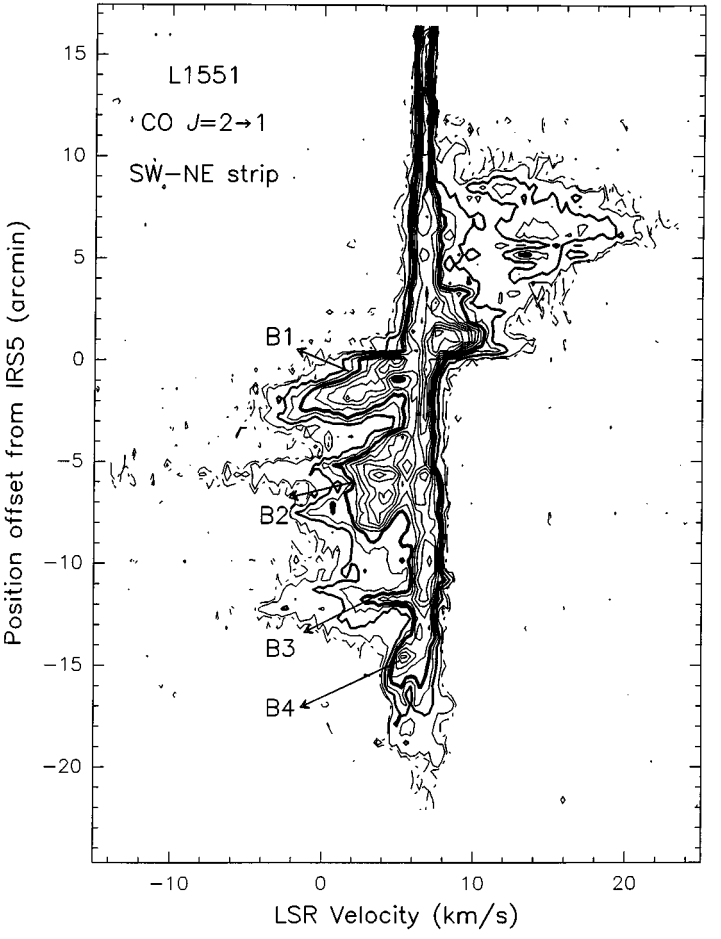

Figure 2 Velocity-position diagram along a line close to the main axis of the L1551 outflow. Position offsets are with respect to IRS5, the outflow exciting source. B1, B2, B3, and B4 are high-velocity features, corresponding to four different lumps of material in the blueshifted lobe of the outflow, which are likely associated with four successive ejection events. (From Bachiller et al 1994a.)

1996), and the HH complexes in L1551 (Mundt & Fried 1983, Snell et al 1980). Surprisingly, some conspicuous HH jets such as HH 34, HH 1/2, HH 46/47, and HH 83, are known to be associated with particularly weak molecular outflows (Chernin & Masson 1991, 1995a; Olberg et al 1992; Bally et al 1994), perhaps because HH jets become optically bright in regions of low visual extinction, in which most of the ambient molecular material has been already dispersed. Recent interferometric images of the HH 111 molecular outflow show that the HH jet lies in a hole of molecular emission, indicating that the jet has cleared out a narrow cylinder in the ambient molecular cloud (Figure 3; Cernicharo et al 1996).

Optical forbidden emission lines also provide powerful diagnostics of bipolar outflows. Observations of the [OI] $\lambda\lambda$ 6300, 6363; [NII] 6583; and [SII] 6716, 6731 Å lines show profiles that are blueshifted with respect to stellar velocity, probably because a thick circumstellar condensation obscures the receding part of the outflow (Mundt 1984; Edwards et al 1987; Appenzeller & Mundt 1989; Cabrit et al 1990; Hirth et al 1994a,b). In addition, the profiles are often double

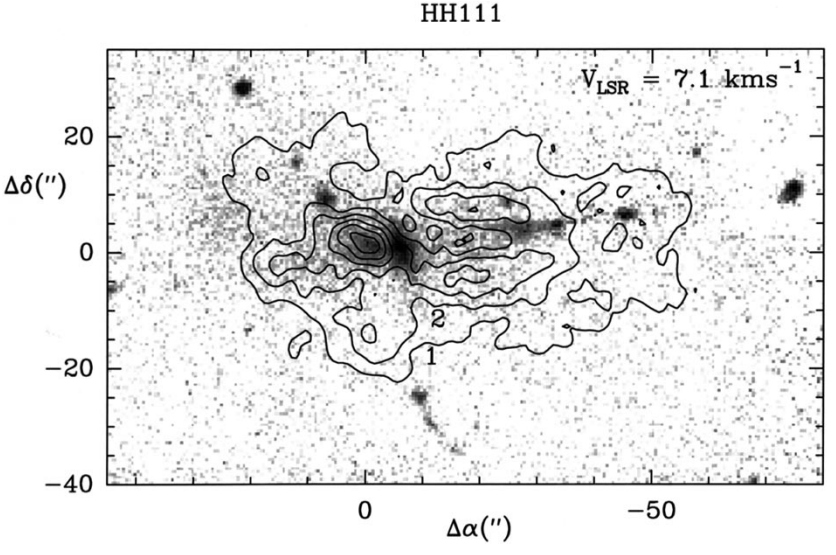

Figure 3 CO 1–0 emission contours superimposed on an H_2 image of the HH 111 region. The CO emission, observed at the Plateau de Bure interferometer, has been integrated in a velocity interval of 0.4 km s^{-1} centered at 7.1 km s^{-1} and traces quiescent ambient material. The H_2 image of the jet was obtained at Calar Alto by J Eislöffel. It appears that the HH 111 jet is clearing up a narrow cylinder in the ambient medium. (From Cernicharo et al 1996.)

peaked with a high-velocity component (HVC, at velocities < -100 km s^{-1}), and a low-velocity component (LVC, at > -30 km s^{-1}). There is observational evidence that the HVC arises from a highly collimated jet from the very vicinity of the star, while the LVC could originate in a wind at the circumstellar disk surface (Kwan & Tademaru 1988; Hirth et al 1994a,b).

Continuum emission at centimeter wavelengths was detected in the early 1980s towards the energy sources of some outflows (Cohen et al 1982, Bieging et al 1984, Bieging & Cohen 1985). Presently about 40 sources have been detected, 10 of which have been imaged (Rodríguez 1995). The maps reveal weak, well-collimated jets emerging from the YSOs. For instance, in the HH 80/81 system in Sagittarius (Reipurth & Graham 1988), a very narrow jet of 5 pc in length is found to be centered on the exciting source (Rodríguez & Reipurth 1989; Martí et al 1993, 1995). In the case of HH 1/2 the HH objects are well detected, and the source spectral index is characteristic of an ionized wind (Pravdo et al 1985). In most cases, the cm-wavelength emission is interpreted as free-free emission from a thermal jet (Reynolds 1986). In addition, spectral indices characteristic of nonthermal synchrotron emission have been derived toward the lobes of the YSO Serpens/FIR1 (Curiel et al 1993) and in the large arcs known as "Orion streamers" (HH 222) emerging from a faint near-IR source (Yusef-Zadeh et al 1990). The coexistence of thermal and nonthermal radio emission in YSO jets has been modeled by Henriksen et al (1991), who suggest that the nonthermal emission is due to relativistic electrons possibly accelerated by a diffusive shock at the region of interaction between the jet and the ambient cloud material.

It is unclear whether the observed (optical and/or radio) jets can drive the associated molecular outflows. Cabrit & Bertout (1992) found a good correlation of the 6-cm luminosity with the force and the luminosity of the associated CO outflows, which in principle argues in favor of the jets driving the outflows. However, Mundt et al (1987) claimed that the momentum of HH jets is not large enough, but momentum estimates are very uncertain because the optical jet densities are difficult to determine (e.g. Raga 1991, Ray 1993). The ejection velocity of the HH jets may also be time-variable (e.g. Raga & Kofman 1992). Thus estimates of the total HH jet momentum might need to be revised. Moreover, as suggested by Parker et al (1991), the lifetimes of the CO outflows could be much greater than their kinematic time scales, and the required momentum injection rate from a possible driving jet could be reduced accordingly. Finally, the possibility remains that a significant neutral (atomic or molecular) component coexists with the ionized jet, helping to drive the molecular SHV outflow. In such a case, the correlation found by Cabrit & Bertout (1992) could be due to a nearly constant ionization fraction in the winds of their YSO sample.

2.3 *Atomic Neutral Component*

The possibility of there being a high fraction of neutral matter in the primary wind appears as one of the most appealing recent suggestions (e.g. Natta et al 1988). Observations of the HI 21-cm line around a few low-mass YSOs such as HH 7–11/IRS, L1551/IRS, and T Tau (Lizano et al 1988, Giovanardi et al 1992, Rodríguez et al 1990, Ruiz et al 1992) have revealed broad wings indicative of winds of up to 200 km s^{-1} and mass-loss rates of 10^{-6} to $10^{-5}\ M_{\odot}\ yr^{-1}$. HI emission has also been detected in two high-mass bipolar outflows (NGC 2071, Bally & Stark 1983; DR21, Russell et al 1992). However, other searches for high-velocity HI emission have failed in some important objects such as L1448 (LM Chernin, private communication, 1994). Such HI observations are always hampered by the relatively poor angular resolution of the cm single-dish telescopes and the confusion of the background Galactic emission.

Certainly, some HI could be created from the dissociation of ambient molecular gas in the shocked regions. But the HI emission could also trace fast and mostly neutral winds, which could in principle drive the CO outflows by entraining ambient material in a mixing layer similar to that modeled by Cantó & Raga (1991) in the context of HH jets. Models of mixing layers more suited for the CO outflows have recently been considered by Lizano & Giovanardi (1995), who estimated the temperature in the mixing layers to be around 4000 K. H_2 is expected to be the main coolant in the layer, and its near-IR line emission is in fact detected toward a high number of CO outflows (see next subsection).

Unfortunately, from the existing observations it is impossible to know whether the high-velocity HI emission arises from a jet, because the poor angular resolution single-dish observations of the HI 21-cm line do not reveal the structure of the neutral atomic component. Lizano & Giovanardi (1995) proposed that the primary neutral wind in L1551 has the form of a wide-angle, radially directed flow, similar to the model of Shu et al (1991). However, this type of model has been found to be unable to explain some basic characteristics of bipolar CO outflows such as the observed distributions of mass and momentum within the flows (Masson & Chernin 1992, Chernin & Masson 1995b). Thus, if the driving agent of molecular outflows is a neutral wind, it has to be highly collimated. Moreover, the possibility that the CO outflows are driven by jets presents the advantage that the two phenomena of highly collimated jets and poorly collimated CO outflows are unified.

As was mentioned above, the forbidden lines of [OI] near 6300 Å also exhibit broad wings, and the highest velocity part of the emission seems to come from a highly collimated jet (e.g. Hirth et al 1994a). The NaI D line is also detected in T Tauri winds (Mundt 1984, Natta & Giovanardi 1990) However, it is difficult to obtain accurate estimates of the momentum rate from the [OI] and

NaI observations. Finally, a neutral wind is expected to contain a substantial fraction of molecules. Even if the jet were initially atomic, some molecules such as CO and SiO could form in relatively short times (Glassgold et al 1989, 1991), and observations of CO and SiO lines could then help in elucidating the structure of the wind. In fact, Lizano et al (1988) detected EHV emission in CO lines around HH 7–11, and this emission was subsequently found to be in the form of a highly collimated jet (Bachiller & Cernicharo 1990, Masson et al 1990). Similar EHV jets have been detected in other objects (see Section 3), suggesting that these EHV CO jets could be the neutral winds driving the standard CO outflows. Clearly, it is very difficult to distinguish the primary wind actually ejected from the central star/disk system from the high-velocity gas accelerated and processed by shocks. The observations reviewed in Section 3 show that, if not the primary wind itself, the EHV CO outflow is very intimately related to the primary driving agent.

2.4 *Molecular Component: High-Excitation H_2 Emitting Gas*

The vibrational transitions of H_2 arise from energy levels > 6000 K above the ground state; thus H_2 molecules become collisionally excited in dense regions at temperatures of a few 10^3 K. As a consequence, such transitions are good potential tracers of shocked molecular gas. In particular, the $v = 1$–0 and $v = 2$–1 S(1) lines of H_2 at $\lambda\lambda$ 2.122 and 2.247 μm are excited in shocks with velocities in the range 10–50 km s^{-1} (Shull & Beckwith 1982, Draine et al 1983, Smith 1994). At higher shock velocities, H_2 molecules are dissociated. Thanks to the recent development of sensitive detector arrays, it is now possible to explore large regions of the sky in the near-infrared at arcsec resolution. The $v = 1$–0 S(1) line has been observed toward the most conspicuous HH flows, including HH 43 (Schwartz et al 1988), HH 1/2 (Davis et al 1994b), HH 7–11 and 12 (Stapelfeldt et al 1991), CepA/GGD37 (Lane 1989), HH 111 (Gredel & Reipurth 1993, 1994; Davis et al 1994c), OriA (Taylor et al 1984), and many others (e.g. Hodapp & Ladd 1995). The extensive survey by Hodapp (1994) in the K' band, which contains the $v = 1$–0 line, reveals a variety of complex morphologies. In general, the H_2 emission is somewhat correlated with the lower-excitation optical features and can trace weaker shocks not visible in the optical (e.g. HH 46/47, Eislöffel et al 1994). Bow shock morphologies are observed at the head of some outflows. In OriA/IRc2, the H_2 jet-like filaments or "fingers" (Taylor et al 1984, Allen & Burton 1993) also terminate in bow shocks.

One of the main advantages of H_2 observations is that they allow the study of particularly young, optically invisible outflows, which are still deeply embedded within dense cores. Strong H_2 emission is observed around several very young Class 0 YSOs (see Section 4), including L1448-mm (Terebey 1991, Bally et al

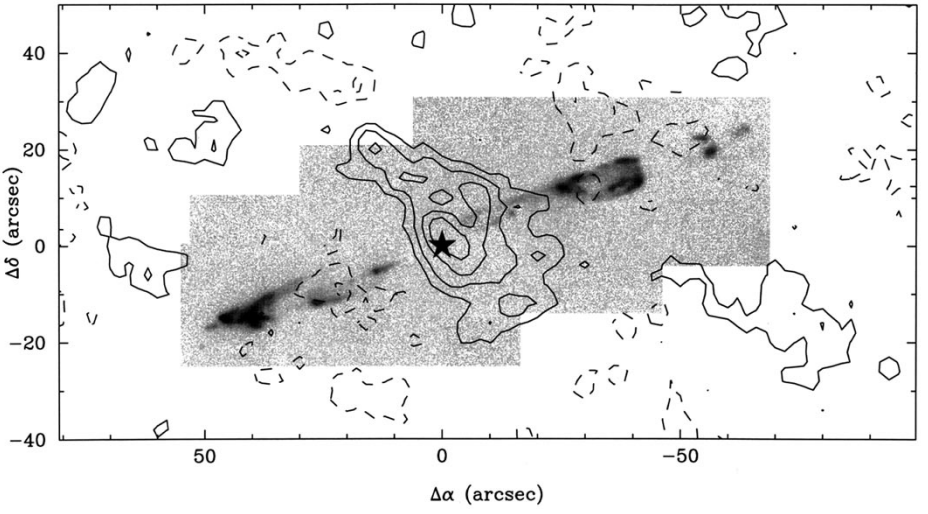

Figure 4 Superposition of a gray-scaled image of the HH 211 jet taken in the H_2 $v = 1$–0 S(1) line at 2.122 μm (from McCaughrean et al 1994) with a NH_3 (1,1) image obtained with the VLA at its D configuration (6″ angular resolution) (R Bachiller & M Tafalla 1995, unpublished data). The star marks the position of the jet source HH 211-mm (see also Table 1).

1993b, Davis et al 1994a), IRAS 03282 (Bally et al 1993a, Bachiller et al 1994b), IC 348-mm (McCaughrean et al 1994), VLA 1623 (Dent et al 1995), and L1157-mm (Hodapp 1994, Davis & Eislöffel 1995). As an example, we show in Figure 4 the jet emerging from IC 348-mm (also called HH 211). The Class 0 source is embedded in a dense NH_3 clump of a few $M_\odot$ (Bachiller et al 1987; R Bachiller & M Tafalla 1996, in preparation). The jet has a kinematical age of < 1000 yr (McCaughrean et al 1994), and the H_2 emission arises in a kind of cocoon around the true jet. This behavior is observed in most of the jets from Class 0 sources: The H_2 emission forms long filaments, but these filaments are not strictly coincident with the axes of the jets. The observations thus confirm that the H_2 line emission arises in the mixing layer where ambient material is entrained. The observation of bow shocks in several sources underscores the importance of the "prompt" entrainment at the jet head (Davis & Eislöffel 1995).

3. HIGHLY COLLIMATED CO OUTFLOWS

The high resolution and sensitivity provided by large millimeter-wave radiotelescopes has resulted in important developments in the study of bipolar outflows. In particular, highly collimated molecular outflows (with collimation factors

> 10) have been recognized as a distinct important class within molecular flows. Well-documented examples are L1448 (Bachiller et al 1990), IRAS 03282 (Figure 1, Bachiller et al 1991c), NGC 2024/FIR5 (Richer et al 1989, 1992), OMC 1/FIR4 (Schmid-Burgk et al 1990), NGC 2264G (Lada & Fich 1996), VLA 1623 (André et al 1990a, Dent et al 1995), and IC 348/HH 211 (McCaughrean et al 1994). Most of these highly collimated flows exhibit extremely high velocity components (in excess of 40 km s^{-1}) concentrated toward the flow axis, and the slower gas is less collimated, similar to the standard CO flows.

3.1 *EHV Components and Molecular Bullets*

In some highly collimated outflows, the CO component on the outflow axis is a jet-like structure flowing at extremely high velocities (i.e. velocities $\sim$ 100 km s^{-1}). Good examples are IRAS 03282 and L1448. The momentum in the EHV jet-like component is large, generally sufficient to put into motion the standard SHV bipolar outflows. In addition, in some particularly clear cases (such as IRAS 03282 and L1448), the terminal velocity of the EHV jet is observed to decrease with distance from the outflow origin, whereas the terminal velocity of the SHV component is observed to increase. This behavior strongly suggests that the EHV jet-like component is injecting momentum into the ambient gas to produce the SHV outflow.

Rather than being a continuous jet, the EHV component presents discrete peaks that are well defined in space and in velocity. Such peaks are referred to as "molecular bullets" (Bachiller et al 1990). An illustrative example is provided by the outflow in IRAS 03282+3035 (Bachiller et al 1991c). Figure 1 shows the structure of the outflow. The EHV jet consists of a chain of molecular bullets interconnected by weaker emission. The standard (SHV) outflow is observed as extended lobes surrounding the EHV jet. Figure 5 shows a few spectra, obtained toward the outflow axis, in which the EHV features are well observed.

Molecular bullets are observed in the majority of highly collimated CO outflows. A remarkable example is that of the HH 7–11 flow. The observed radial velocities of the bullets in this outflow exceed 100 km s^{-1} with respect to the ambient cloud, and their CO linewidths are about 20 km s^{-1} (Bachiller & Cernicharo 1990, Masson et al 1990). Not all molecular bullets in highly collimated jets present such extreme radial velocities. For instance, the CO jet around VLA 1623 (André et al 1990a) also exhibits a clear structure in clumps, but the radial velocities observed toward this jet are ≤ 30 km s^{-1}, probably due to a very high inclination of the outflow with respect to the line of sight. Other highly collimated CO outflows presenting a clear structure with molecular bullets include NGC 2024/FIR5 (Richer et al 1989, 1992), HH 111 (Cernicharo & Reipurth 1996), and IRAS 2005 (Bachiller et al 1995a). The typical sizes of

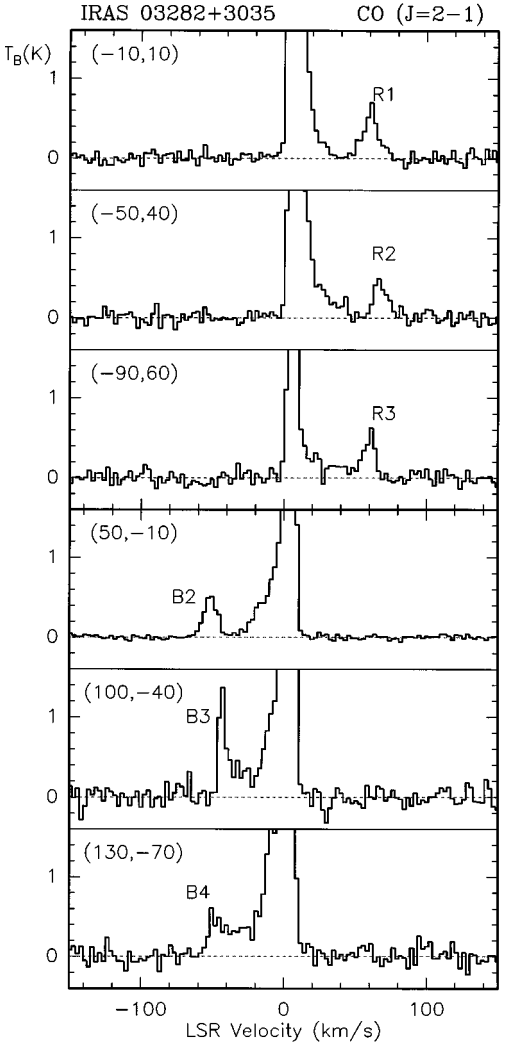

Figure 5 CO 2–1 spectra observed toward selected positions in the IRAS 03282+3035 outflow (from Bachiller et al 1991c). The position offsets (marked in the upper right corner of each panel) are relative to the position of the exciting source (see Table 1). High-velocity molecular bullets are denoted by R1, R2, and R3 (redshifted) and B2, B3, and B4 (blueshifted). Note that the emission extends over a velocity range of about 140 km s^{-1}.

such bullets are a few 10^{-2} pc, and their masses are a few $10^{-4}\ M_\odot$, as derived from multiline CO observations (e.g. Bachiller et al 1990). The kinematic time scales range from a few hundred to a few thousand years.

Molecular bullets tend to be regularly spaced along the axis of the highly collimated jets. In the IRAS 03282 and L1448 outflows (Bachiller et al 1991c, 1990), the bullets can be grouped in symmetrical pairs. The striking symmetry found in position and velocity between the redshifted and the blueshifted bullets indicates that, rather than produced in situ, each pair of bullets corresponds to a bipolar ejection taking place near the central YSO. Such ejection events are quasi-periodic, and the time elapsed between two successive outbursts is of the order of 10^3 yr. Intermittency seems to be a relatively common characteristic of highly collimated outflows.

Discrete high-velocity CO components are also observed in the immediate vicinity of some YSOs with near-infrared spectroscopy (e.g. Mitchell et al 1991), but the relationship of these features to the molecular bullets observed in the rotational CO transitions is unclear. Another phenomenon that could be related with molecular bullets are the successive shocked knots observed in optical and near-infrared jets (Reipurth 1989; Reipurth & Heathcote 1991, 1992; Hartigan et al 1993; Bally et al 1993b; Eislöffel & Mundt 1994). Such shocked knots are also believed to be associated with recurrent ejection events (Reipurth 1989).

The precise origin of the eruptions that cause molecular bullets is not well understood, but it is noteworthy that the masses and time scales of bullets are similar to those of the "optical" outburst observed in FU Ori stars. The FU Ori eruptions can be well explained by a large increase in the accretion rate through a circumstellar disk (Hartmann & Kenyon 1985), up to $10^{-4}\ M_\odot \mathrm{yr}^{-1}$. For an average duration of about 100 yr, this yields a total accreted mass up to $10^{-2}\ M_\odot$. The masses of the molecular bullets would thus be consistent with a ratio of accretion rate to mass outflow of ~ 10 to 100.

The EHV molecular bullets present extraordinary chemical characteristics. For instance, the abundance of the SiO molecules can be enhanced by several orders of magnitude with respect to the quiescent ambient cloud (Bachiller et al 1991b, Guilloteau et al 1992). Chemical reactions in an initially neutral atomic wind seem able to produce significant amounts of SiO (Glassgold et al 1989, 1991). However, the large SiO abundance and its observed spatial distribution in different flows suggest that an important part of the SiO enhancement is produced by shocks associated with the highly collimated outflow (see Section 5).

3.2 *Molecular Bow Shocks*

One of the most intriguing aspects of bipolar outflows is that, in many cases, highly collimated jets coexist with poorly collimated molecular flows. Jets are

usually observed along the axis of wide CO flow lobes that resemble ovoidal or ellipsoidal cavities. How a narrow highly supersonic jet can generate so wide a cavity is a fundamental question addressed by recent observations and models. Interferometry at millimeter wavelengths now makes it possible to image the CO outflows with a resolution close to an arcsec (Sargent & Welch 1993); these data can shed light on this issue. The most detailed observations available so far are those of the L1448 and L1157 outflows. Figure 6 shows a comparison of the H_2 image of L1448 (from Bally et al 1993b) with the images of the slow-moving CO obtained with the IRAM interferometer (Bachiller et al 1995b). The H_2 images reveal a series of well-defined bow shocks in the blueshifted lobe, whereas the slow-moving molecular gas traces the edges of a biconical limb-brightened cavity. The blueshifted part of the cavity is also seen in the continuum near-infrared emission, which is scattered at the cavity walls (Bally et al 1993b). It is remarkable that the walls of the CO cavity seen at blueshifted velocities (top left panel in Figure 6) seem to be complementary to the bow shock H_2 structure, which is the closest to the exciting source, L1448-mm. The arc structure delineated by the H_2 emission seems to close the conical CO cavity. This configuration strongly suggests that the large opening angle of the SHV CO outflow results from the entrainment of ambient material through the large bow shocks traced by the H_2 line emission.

Another example of a bow shock–driven outflow is that in L1157 (Umemoto et al 1992, Gueth et al 1996). Figure 7 shows velocity channel CO images of the blueshifted lobe. The images reveal at least two prominent limb-brightened cavities, which also seem to be created by the propagation of large bow shocks. These observations also illustrate the importance of combining single-dish data with the interferometric data. In fact, with only the purely interferometric images (top row of the figure), one could think that the cavities are empty structures. When one adds the zero-spacing information (middle row), significant CO emission arising from the inner part of the cavities becomes evident. The bow shocks at the head of the cavities are also well observed in NH_3 emission (Bachiller et al 1993), and VLA images reveal a structure similar to that seen in CO (M Tafalla & R Bachiller 1995; 1996, in preparation; see below).

Figure 6 Superposition of a gray-scaled H_2 image of the L1448 jet (from Bally et al 1993b) and the interferometric images of the CO 1–0 emission integrated over four intervals at low velocities (from Bachiller et al 1995b). The central LSR velocity for each interval is given at the upper left corner of each panel. First contour and step are 0.92 K km s^{-1}. The jet direction, defined by SiO observations, is indicated by the solid line. The positions of L1448-mm and IRS3 are marked with stars. A part of the CO outflow from IRS3 is visible in the 7 km s^{-1} panel. The H_2 emission traces large bow shocks, whereas the CO delineates the walls of a biconical cavity. Note that the walls of the CO cavity in the blueshifted lobe are complementary of the first H_2 bow shock. This morphology strongly suggests that the CO bipolar outflow results from entrainment of ambient material through the propagation of large bow shocks.

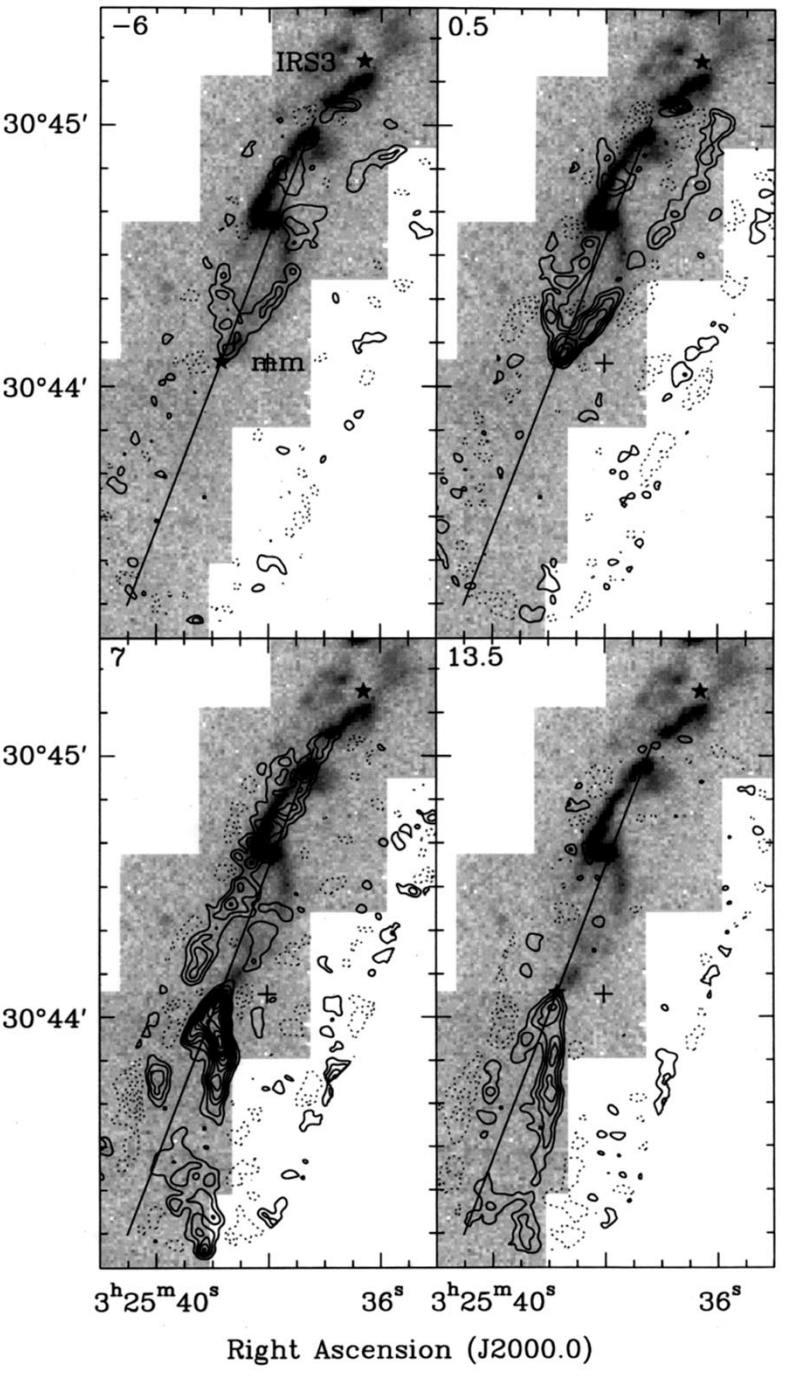

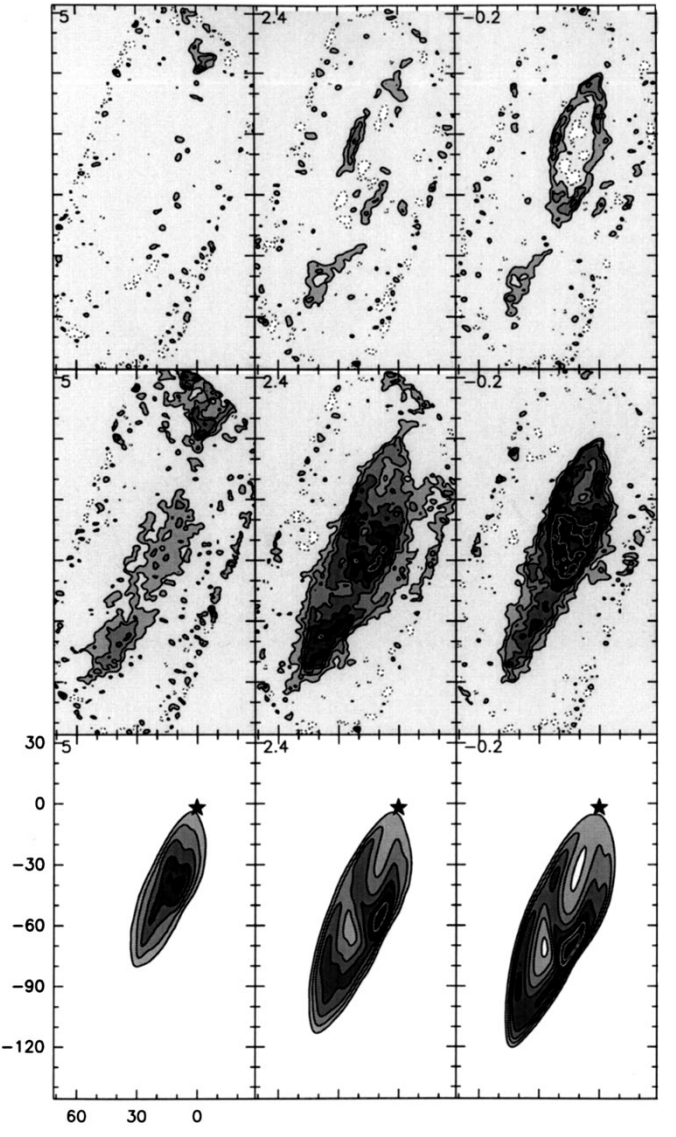

Figure 7 CO emission from the blueshifted lobe of the L1157 outflow integrated over velocity intervals of 2.6 km s^{-1}. The central LSR velocity for each interval is given at the upper left corner of each panel. The LSR velocity of the ambient gas is 2.75 km s^{-1}. Position offsets are in arcsec with respect to the L1157-mm (see Table 1), whose position is indicated with a star. First contour and step are 155 mJy/beam (1.3 K). The beam size is $3.6'' \times 3''$ at P.A. 90°. (*Top row*) CO 1–0 maps reconstructed from purely interferometric IRAM data. (*Middle row*) Images obtained after inclusion of the short spacing information obtained at the IRAM 30-m telescope. (*Bottom row*) Synthetic maps obtained with a precessing, episodic jet model smoothed to the resolution of the observations. (Adapted from Gueth et al 1996.)

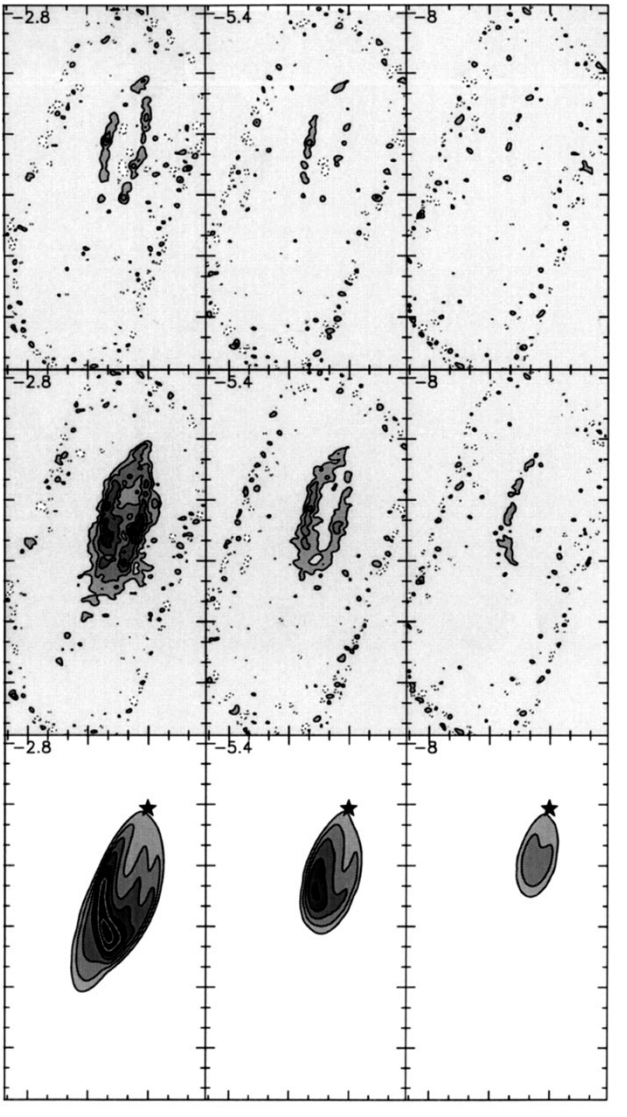

Figure 7 (*continued*)

Interestingly, the two cavities are not well aligned on a single line passing through the exciting source, L1157-mm, as if the axis of the underlying jet had precessed from the first ejection event to the second one. A simple spatio-kinematic model in which the jet precesses on a narrow cone (of opening angle close to 6°) provides an accurate description of the observations (bottom row of the figure). Thus, the large opening angle observed at the base of the CO outflow is very likely determined by the large size of the propagating bow shocks, rather than to the jet precession, which happens in a very narrow cone.

In more massive objects, higher confusion makes the identification of molecular bow shocks more difficult and also complicates the association of the bow shocks with the CO outflows. In the case of Orion/IRc2, multiple H_2 bow shocks are observed to emerge from the central source (Taylor et al 1984, Lane 1989, Allen & Burton 1993), forming a wide fan. However, the comparison with the SHV CO outflow is difficult in this case because of the confusion with the possible interaction of the molecular cloud with the extended HII region in the background (Rodríguez-Franco 1995). Finally, it is interesting to note that the H_2O maser features in W49 (Gwinn et al 1992) seem to delineate the surfaces of an elongated cocoon produced by a jet (Mac Low & Elitzur 1992, Mac Low et al 1994).

3.3 *What Drives the High-Velocity Gas?*

As mentioned above, a wind emanating from the central star/disk system was soon proposed as the primary physical agent that could drive the observed CO outflows (Snell et al 1980, Lizano et al 1988, Shu et al 1991). However, wide-angle winds fail to explain some important properties of molecular outflows, such as the observed amount of mass as a function of velocity (Masson & Chernin 1992). In fact, low-collimation winds would contain more material at extreme velocities than observed in actual outflows. Jets, on the other hand, can sweep the gas aside by means of bow shocks, and most of the gas would be at low velocities, in agreement with observations. Wide-angle winds are also unable to explain the observed spatial distribution of momentum in molecular outflows (Chernin & Masson 1995b) and the morphology of the highly collimated CO outflows (see discussion above). Thus, the primary driving agent of molecular outflows is very likely a jet. As mentioned above, a great advantage of the jet-driven picture is that it unifies two phenomena, HH jets and CO outflows, that were initially considered intrinsically different.

When a jet interacts with the ambient molecular medium, the shock is unlikely to be adiabatic (energy conserving), owing to fast cooling. In fact, diffuse far-infrared emission is observed in L1551 with a morphology similar to that of the outflow, and the far-infrared luminosity is about 18% of the bolometric luminosity of the central YSO (Edwards et al 1986, Clark & Laurejis 1986).

In the case of HH 46/47, the luminosity in the H_2 lines is comparable to the mechanical power of the CO outflow (Eislöffel et al 1994). In addition, the high bipolarity observed in some outflows makes the energy-conserving winds implausible for producing outflows (Meyers-Rice & Lada 1991, Lada & Fich 1996). Thus, outflows are likely driven in a momentum-conserving fashion. The transfer of momentum from the jet to the ambient medium can be achieved in different ways (see e.g. Dyson 1984). From numerical hydrodynamical simulations, De Young (1986) distinguished two basic processes: 1. the "prompt entrainment" happening at the head (bow shock) of the jet and 2. the "steady-state entrainment" taking place along the sides of the jet by turbulent mixing of the ambient material through Kelvin-Helmholtz instabilities. The numerical simulations (De Young 1986) show that the first process dominates in the case of intermediate Mach number jets ($M = 5$–10), with internal densities comparable to that of the external medium. Turbulent steady-state entrainment is the dominant process in low-velocity jets ($M \sim 1$).

Specific models for stellar jets were first developed to account for the observations of HH jets (Raga 1988, Tenorio-Tagle et al 1988, Blondin et al 1990, Gouveia dal Pino & Benz 1993, Hartigan & Raymond 1993, Stone & Norman 1994). These models are mainly concerned with the propagation of the jet itself, and they do not consider the possible generation of molecular flows through the entrainment of quiescent ambient material. Recently, attempts have been made to specifically model the creation of CO outflows by jets. Such jet-driven outflow models are still very approximate and do not intend to provide a full description of all the complex hydrodynamical phenomena involved. The models can be classified in two families, depending on the entrainment process assumed to be mainly responsible for the CO outflow.

Turbulent entrained outflow models (Stahler 1993, 1994; Raga et al 1993b) emphasize the steady-state turbulent entrainment. Such models seem to explain the velocity shear structure observed at the base of some outflows such as IRAS 03282 (Tafalla et al 1993b); they could also explain the "Hubble law" observed in many outflows (Stahler 1994; but see also Lada & Fich 1996). However, the observed low collimation of CO outflows in not well understood in this model, since the width of the boundary mixing layer in which the entrainment of ambient material (the CO outflow) occurs is expected to be very thin, comparable to the jet radius (Cantó & Raga 1991, Raga et al 1993b).

Bow shock outflow models aim to explain the production of the CO flows by prompt entrainment (Masson & Chernin 1993, Raga & Cabrit 1993, Chernin et al 1994b). In fact, prompt entrainment through bow shocks is the expected dominant process in outflows, owing to the high Mach numbers ($M > 10$). Narrow jets could, in principle, produce much larger bow structures, which

would explain the coexistence of the highly collimated jets with the poorly collimated CO flows. In fact, as discussed above, large bow shocks are directly observed by their line emission in many sources. Bow shocks are able to sweep up large amounts of ambient material (Masson & Chernin 1993), conserving momentum. However, not all the observed details are well accounted for by the existing bow shock outflow models. For instance, the existing models (e.g. Raga & Cabrit 1993) fail to reproduce the shapes of the cavities excavated by the propagation of the bow shocks (Gueth et al 1996), and the observed spatial distribution of momentum cannot be accounted for (Chernin & Masson 1995b). But it is important to note that the Raga & Cabrit model is made for an "internal working surface," and not for a "leading jet head." This model also assumed that the passage of the bow shock will be followed by a turbulent wake, but at the present time it is unclear what kind of velocity field is expected in this complex region. Finally, the existing numerical models of bow shocks (Stone & Norman 1994, Chernin et al 1994b) predict bow structures that are narrower than what is necessary to explain the wide opening angles of CO outflows. Jet precession has been argued as a possible mechanism to broaden the outflow lobes (Masson & Chernin 1993), but the observational studies of precession in CO flows are difficult due to the complex morphologies of the lobes, and in the most promising cases for precession, the width of the CO lobes seems to be caused by large bow shocks (Figure 7, Gueth et al 1996).

In conclusion, bow shock outflow models seem to be the most promising ones for explaining most of the observational characteristics of CO outflows, but future models should address the problem of the large transverse sizes of the observed CO lobes and bow shocks. In addition, turbulent entrainment could still efficiently operate in some regions (or at some evolutionary stages) of the jet/outflow system. As discussed above, the observed jets are clearly eruptive, and first attempts have been made to model time-variations in velocity, mass-loss rate, and angle of ejection in bipolar outflows (Raga & Kofman 1992, Hartigan & Raymond 1993, Biro & Raga 1994, Raga et al 1993a). Clearly, time-variability is a dominant aspect of molecular outflows, and future models should take it into account.

4. CHEMISTRY

Shocks are the natural result of the propagation of high-Mach-number outflows within molecular clouds. Shock waves compress and heat the gas, triggering chemical reactions that do not operate in quiescent environments. In addition, shock processing of the dust grains results in the injection of some particular atoms and molecules into the gas phase. Thus the molecular gas in the vicinity of YSOs is expected to present a distinct and unusual chemical composition.

Some molecular abundances are known to be enhanced as a result of the action of bipolar outflows on the surrounding gas. Observations of the outflow around OriA/IRc2 have provided valuable information about the chemical processes activated by the birth of a high-mass star in the surrounding medium. Evaporation of molecules from dust grains and high-temperature shock chemistry have been found to be important processes in increasing the abundances of some sulfur, oxygen, nitrogen, and deuterium compounds (Plambeck et al 1982; Blake et al 1987; Plambeck & Wright 1987; Walmsley et al 1987; see Rodríguez-Franco 1995, for a complete review). Unfortunately, the case of OriA/IRc2 is particularly complex owing to the presence of at least five gas components (the outflow, the expanding "doughnut," the hot core, the ridge, and the compact ridge) of different physical conditions along the line of sight.

Important chemical effects have also been observed in some outflows from low-mass YSOs, which usually present much less confusion than OriA/IRc2. One of the most extreme examples is SiO, whose abundance is enhanced by several orders of magnitude at the heads and along the axes of some molecular outflows (Bachiller et al 1991b, Martín-Pintado et al 1992, McMullin et al 1994a). Other molecules with well-documented outflow enhancements include SO (Martín-Pintado et al 1992, Schmid-Burgk & Muders 1995, Chernin et al 1994a), NH_3 (Bachiller et al 1993, Tafalla & Bachiller 1995), and CH_3OH (Bachiller et al 1995c, Sandell et al 1994). As an example, the NH_3 (3, 3) line near λ 1.3 cm is dominated by broad emission around the L1157 outflow, and it becomes possible to image the flow with the VLA. Recent images obtained in its D configuration (5″ angular resolution) reveal a structure of successive bow shocks along the outflow axis (Figure 8; M Tafalla & R Bachiller 1995; 1996, in preparation).

Interest in detecting molecular lines from shocked regions not only comes from the chemistry involved but also from the fact that molecular lines provide a very useful tool for estimating the physical conditions of the shocked component. The case of ammonia is particularly important, since this is the best interstellar thermometer. Additionally, multiline studies of SiO and CH_3OH allow reliable estimates of the volume densities. For instance, in the bow shock associated with the L1157 blueshifted outflow, the kinetic temperature has been estimated to be 80 K and the volume density to be a few 10^6 cm^{-3} (Bachiller et al 1993, 1995c). It thus appears that the shocked gas traced by the mm molecular lines is not as hot as the gas traced by the near-infrared lines of H_2 (which is at a temperature of a few 10^3 K).

Modeling the complex shock chemistry operating in the vicinity of YSOs requires estimating a relatively large number of molecular abundances. Such estimates should be done through extensive molecular line surveys at millimeter

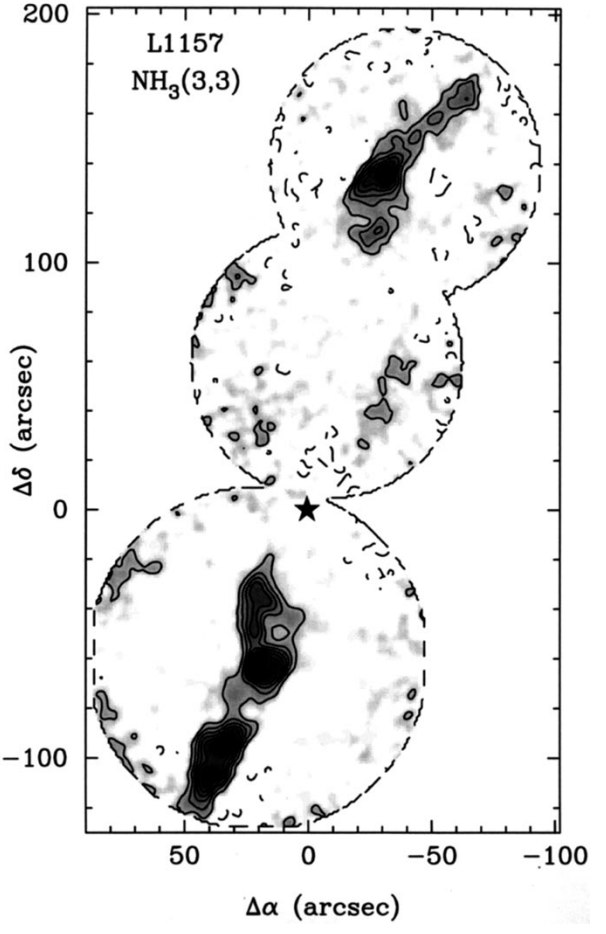

Figure 8 Integrated intensity map of the NH_3 (3, 3) line emission in the L1157 outflow obtained with the VLA (D configuration, 5″ resolution). The northern lobe is redshifted emission; the southern one is blueshifted. The map center is on L1157-mm (see Table 1), the outflow exciting source. The NH_3 (3, 3) line traces warm gas ($T \sim 70$ K) associated with bow shocks. Data are from Tafalla & Bachiller (1995), augmented with recent unpublished observations by the same authors.

wavelengths. The vicinity of low-mass YSOs are the best targets for these kinds of studies, because the confusion in these regions is expected to be less severe than in more massive clouds. The first extensive millimeter surveys have been carried out toward the Class 0 sources NGC 1333/IRAS 4 (Blake et al 1995) and IRAS 16293 (Blake et al 1994, van Dishoeck et al 1995). Figure 9 shows some results from one of these surveys toward the L1157 outflow. The chemical segregation in this cloud is particularly illustrative. The narrow line profiles observed toward the position of the source arise from cold quiescent gas, whereas toward the bow shock region the profiles are dominated by the broad lines associated with the shock. Some molecular lines such as those of DCO^+ and N_2H^+ are only observed toward the cold gas condensation around the exciting source, whereas some other molecules such SiO and methanol (CH_3OH) only trace the hot warm gas in the shock. CS and H_2CO lines are observed in both gas components (R Bachiller et al 1996, in preparation).

The detailed chemical processes induced by the action of shocks are poorly understood. In most cases, the emission of shock-chemistry molecules is seen at the position of the bow shocks [e.g. IRAS 03282 and L1157 (R Bachiller et al 1994b; 1996, in preparation)], but SiO emission is also seen arising from shocks *along* the highly collimated molecular outflow in L1448 (Bachiller et al 1991b, Guilloteau et al 1992, Dutrey et al 1996). It seems clear that SiO is a result of the shock chemistry following the destruction of the refractory grain cores. However, other molecules such as ammonia and methanol, which are known to be abundant in the ice dust mantles (e.g Allamandola et al 1992), could be directly desorbed from them. Deuterated species could also be removed from the grains by grain-grain collisions (van Dishoeck et al 1995). The origin of other molecules such as SO and HCO^+ is even less clear. Theoretical studies of the outflow chemistry should include a high number of processes, namely the effect of the UV near HH objects (Wolfire & Königl 1993), the chemistry of the atomic component in the jet (Glassgold et al 1989, 1991), the mixing layer chemistry (Taylor & Raga 1995), as well as the specific processes related to the shocks (e.g. Iglesias & Silk 1978, Neufeld & Dalgarno 1989, Millar et al 1991, Pineau des Forêts et al 1993).

5. DRIVING SOURCES

Most of the driving sources of bipolar molecular outflows are YSOs that are deeply embedded within the molecular cores in which they were born. YSOs are difficult to classify in a scheme such as the H-R diagram because they do not radiate as single blackbodies. Rather, their spectral energy distributions (SED) are often broad, resulting from the wide range of temperatures in their dusty envelopes (e.g. Scoville & Kwan 1976). Spectral types are also difficult to

assign due to the strong obscuration, although near-infrared spectroscopy seems to be a promising tool (Hodapp & Deane 1993, Casali & Eiroa 1995). However, as protostellar outflows disperse the material surrounding the YSO, a systematic change in the SED is produced (see, e.g. Shu et al 1987), and this evolution of the SED shape can be used to classify the YSOs in different evolutionary classes (see below). Understanding the mechanisms of dispersion of the dense circumstellar gas around YSOs is also of crucial importance because this dispersion will probably determine the final mass of the star/disk system that is under formation.

5.1 *Core Disruption and the Classification of YSOs*

Dense cores harboring outflows are known to present broader NH_3 lines than nonoutflow cores (Myers et al 1988), but the nature of the line broadening mechanism is not well understood. Turbulence and systematic motions such as rotation, infall, and expansion have been proposed as possible causes of line broadening. However, in most cases of outflow cores that have been properly mapped in lines tracing high-density material, the velocity fields traced by these lines clearly reflect the outflow motions. Some examples are NGC 6334I (Bachiller & Cernicharo 1990), CepA (Bally & Lane 1990, Torrelles et al 1987), NGC 2071-N (Iwata et al 1988), L1551 (Menten & Walmsley 1985; M Tafalla & PC Myers 1996, in preparation), and the dense cores in the L1204/S140 (Tafalla et al 1993a). In some of these cases the velocity field, when studied with low resolution or sensitivity, was first interpreted as rotation, but further high-sensitivity observations revealed the association of the core velocity field with the outflow. In Figure 10 we summarize the situation observed in the L1228 dense core (from Tafalla et al 1995). In this core, the embedded source IRAS 20528+7724 drives a powerful CO outflow of 1.3 pc size (Bally et al 1995). The dense gas exhibits bright lines of C_3H_2 in a region of 0.1 pc around the IRAS source. The middle panels in Figure 10 show the velocity structure within the dense core by using three velocity channel maps of 0.5 km s^{-1} width. The blueshifted and redshifted emissions show no overlap and clearly reflect the outflow motion. The spectra observed at the positions B, R, and C (bottom panel of the figure) show that the entire line profile is shifted, by a full linewidth,

Figure 9 Spectra obtained toward two representative positions of the L1157 outflow. The (0, 0) position is that of the exciting source L1157-mm (see Table 1), whereas the ($20''-60''$) position is one of the prominent bow shocks in the blueshifted lobe (see e.g. Figure 8). Note the differences in the behavior of the different molecular lines. Some molecules (such as N_2H^+ and DCO^+) only trace the quiescent gas associated with the dense core, whereas other molecules (e.g. SiO, CS, H_2CO, CH_3OH) show broad emission associated with the outflow. [From R Bachiller et al (1996, in preparation).]

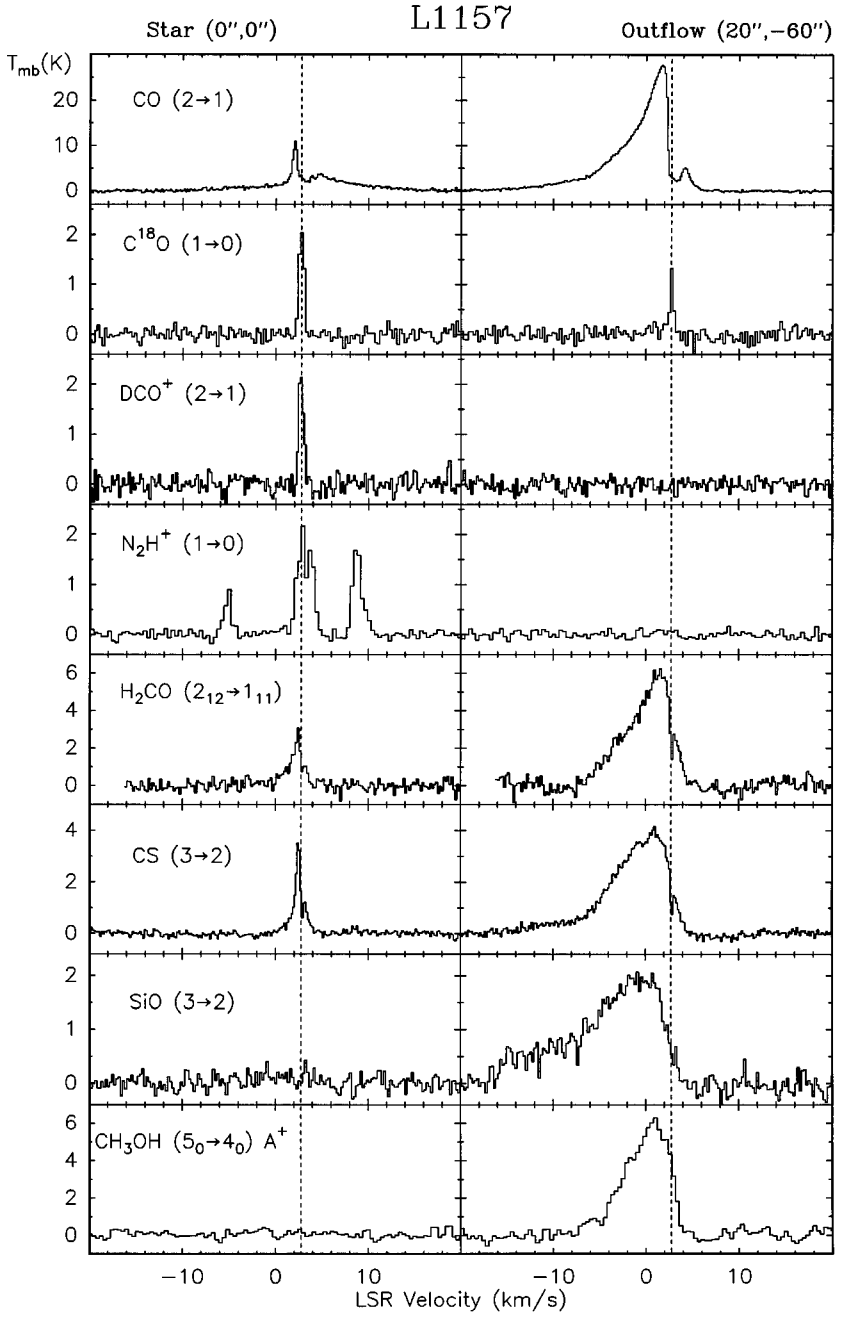

from one position to the other. The outflow seems to accelerate fragments of the dense core to velocities higher than the internal velocity dispersion. In this way, outflows can excavate cavities in dense cores, producing bipolar nebulae that will successively become visible in the near-IR [as in the case of L1448 (Bally et al 1993b, Bachiller et al 1995b)] and finally in the optical (such as NGC 2261, Hubble's variable nebula around R Mon).

As the circumstellar material is dispersed around a YSO by the action of the outflows, the SED of the YSO will systematically evolve. This process allows one to classify the YSOs in Classes I, II, and III, depending upon the value of the infrared spectral index [$\alpha_{\rm IR} = -d\,\log(\nu F_\nu)/d\,\log\nu$] evaluated longward of 2.2 μm (Lada & Wilking 1984, Adams et al 1987, Lada 1991). Class I sources have $\alpha_{\rm IR} > 0$ and SEDs broader than single blackbody functions, probably resulting from warm (300–1000 K) dusty envelopes around a hot (3000–5000 K) stellar-like object. These sources are associated with dense molecular cores (Myers et al 1987). Class II sources have $\alpha_{\rm IR} < 0$ and again SEDs broader than a single temperature blackbody. They are optically visible and exhibit spectra similar to those of cool photospheres, i.e. they are probably classical T Tauri stars surrounded by dusty disks. Class III sources have $\alpha_{\rm IR} < 0$, SEDs similar to those of single blackbodies, are visible, and do not exhibit large infrared excess. They include pre–main sequence stars surrounded by optically thin disks, very young stars of the main sequence, and "naked" T Tauri stars (Walter et al 1988).

In addition to these sources, recent observations with bolometers at millimeter wavelengths have revealed the existence of colder sources that do not fit in the classification scheme depicted above. Such objects, called "Class 0" sources, are thought to be in an evolutionary stage prior to Class I; these are described in the next subsection. The SEDs of these different classes of sources have been successfully modeled by assuming a systematic dispersal of the total circumstellar mass from Class 0 to Class III (Adams et al 1987, Kenyon et al 1993), and it is believed that the circumstellar mass decreases by a factor of 5–10 from one class to the next (André & Montmerle 1994).

In an attempt to describe the evolution of YSOs and main-sequence stars in a unified way, Myers & Ladd (1993) introduced a parameter called bolometric

Figure 10 Interaction of the molecular outflow with the dense core in L1228. (*Top panel*) Integrated intensity of the CO high-velocity gas superimposed to the C_3H_2 emission, which traces the core. (*Middle panel*) C_3H_2 emission from within the box marked in the upper panel, integrated over three velocity intervals 0.5 km s^{-1} wide. A clear bipolarity is observed in the kinematics of the core. (*Bottom panel*) C_3H_2 spectra from the positions B, C, R indicated in the top panel. A velocity shift in the line profiles is observed from each position to the next. (Adapted from Tafalla et al 1995.)

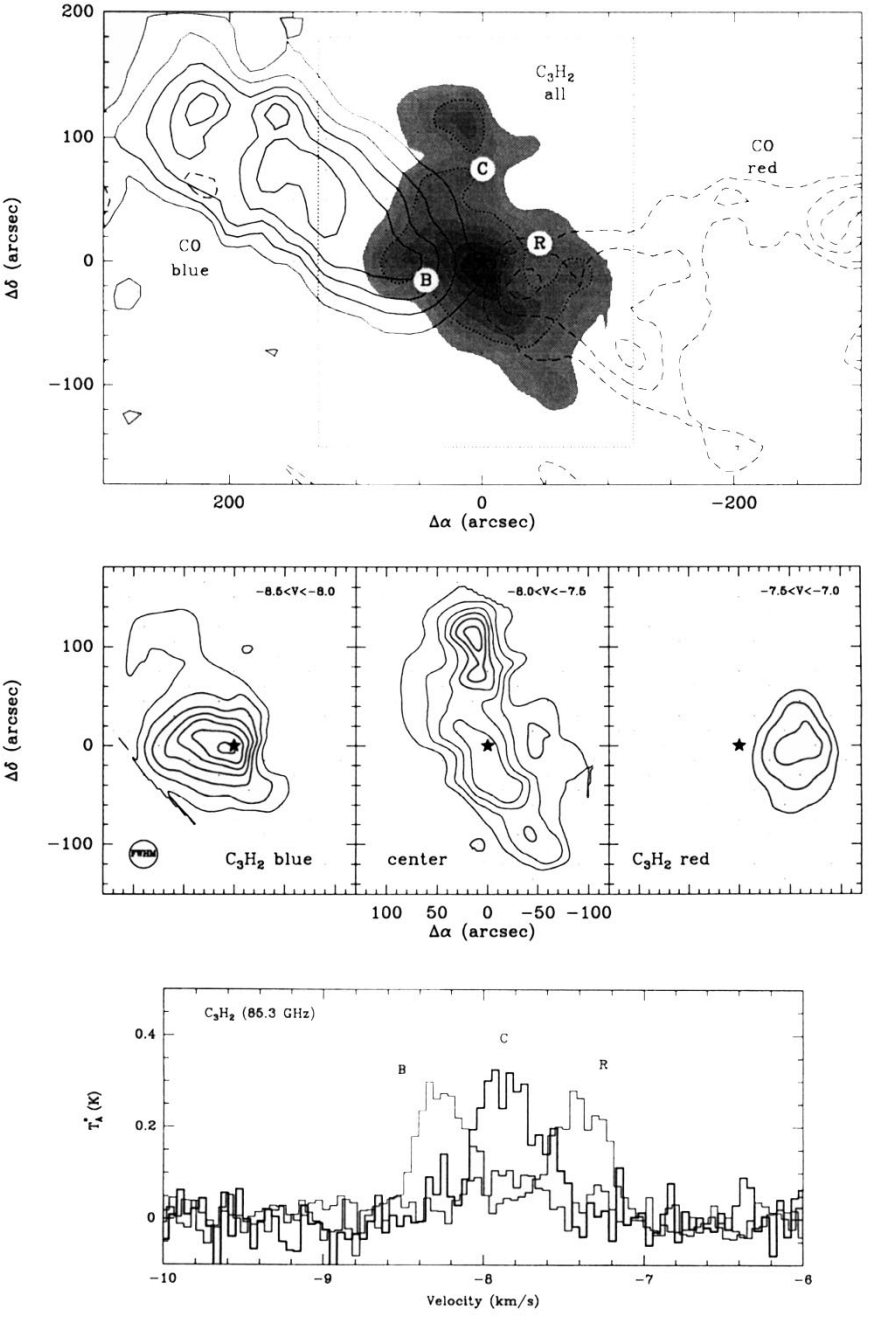

temperature, $T_{\rm bol}$, the temperature of a blackbody having the same mean frequency as the observed SED. $T_{\rm bol}$ increases monotonically from Class 0 objects to classes I, II, and III, corresponding to the SED evolution. Class 0 sources have $T_{\rm bol} < 100$ K, whereas typically $T_{\rm bol} \sim 700$ K in Class I sources, ~ 2000 K in Class II, and ~ 3500 K in Class III. The bolometric temperature seems to be an appropriate parameter to describe the different kinds of YSOs, because it uses all the available SED information, and it can be used for the whole range of YSO classes. In addition, the log-log diagram of $L_{\rm bol}$ vs $T_{\rm bol}$ (the BLT diagram) is the analog for YSOs to the H-R diagram, with the advantage that both diagrams have the same main sequence. The BLT diagram can be used to compare observations with theoretical evolutionary models and for comparative studies of different star-forming regions (Chen et al 1995).

5.2 *Class 0 Protostars*

One of the most interesting issues addressed in the study of YSOs is the identification of protostars. Recent observations at millimeteter wavelengths (André & Montmerle 1994) have shown that a YSO at the Class I stage has already assembled most of its stellar mass (i.e. the mass of its circumstellar envelope is well below its stellar mass: $M_{\rm CE} < M_*$). However, in protostars, i.e. objects in which the luminosity is generated from the gravitational accretion, one expects that the stellar mass has not been fully accumulated ($M_{\rm CE} > M_*$). Such pre–Class I objects are referred to as "extreme Class I" sources (Lada 1991) or "Class 0" protostars (André et al 1993). The evolutionary sequence from Class 0 to III is summarized in Figure 11. Pre-protostellar cores prior to the start of gravitational collapse can be identified by mapping the millimeter/submillimeter emission in dark clouds (Benson & Myers 1989, Ward-Thompson et al 1994).

Phenomenologically, a Class 0 protostar is defined as a submillimeter source with the three following attributes (André et al 1993, Barsony 1995): 1. At most, weak emission at $\lambda < 10$ μm, 2. a spectral energy distribution similar to a blackbody at 15–30 K, and 3. $L_{\rm submm}/L_{\rm bol} > 5 \times 10^{-3}$, where $L_{\rm submm}$ is the luminosity measured at $\lambda > 350$ μm and $L_{\rm bol}$ is the bolometric luminosity. In addition, Class 0 protostars can be observationally distinguished from pre-protostellar cores by the presence of a centimeter source (ionized gas) or an outflow. Table 1 lists most of the Class 0 sources identified at present, together with some of their characteristics.

Gravitational infall is expected to occur in Class 0 sources, and spectral lines of moderate optical depth should show the redshifted self-absorption asymmetry characteristic of infall motions. However, the velocity field around YSOs is often complicated by the presence of outflow motions, and the observed line profiles are complex. In some cases, nevertheless, the evidence for infall seems well founded, namely in B335 (Zhou et al 1993), IRAS 16293 (Walker et al

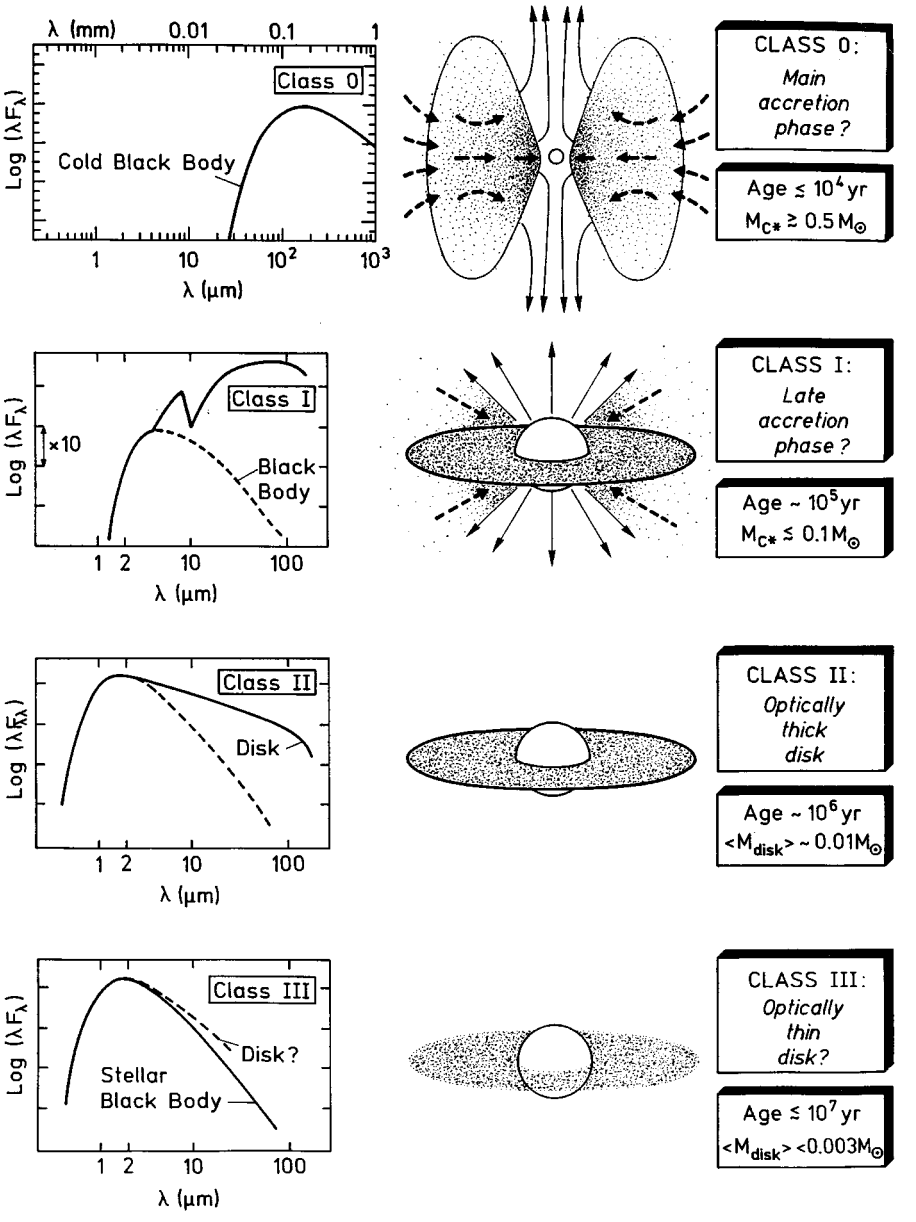

Figure 11 Evolutionary sequence of the spectral energy distributions for low-mass YSOs as proposed by André (1994). The four classes 0, I, II, and III correspond to successive stages of evolution.

Table 1 Properties of candidate Class 0 protostars

Source	IRAS name	α(1950.0)	δ(1950.0)	Dist. (pc)	L_{bol} ($L_\odot$)	M_{env} ($M_\odot$)	T_d (K)	Outflow[a]	Ref.[c]
L1448-mm		03 22 34.3	30 33 35	300	10	2	30	hc	1, 2, 3
L1448/IRS3	03225+3034	03 22 31.5	30 34 49	300	9	1.4		hc	1, 3
NGC1333/IRAS2*		03 25 49.9	31 04 16	350	40			hc,mu	4, 5
NGC1333/IRAS4A		03 26 04.8	31 03 13	350	14	7	37	hc	5, 6
NGC1333/IRAS4B		03 26 06.5	31 02 51	350	14	3		bip	5, 6
IRAS03282	03282+3035	03 28 15.2	30 35 14	300	2	0.6	26	hc	7, 8
HH211-mm		03 40 48.7	31 51 24	300	$\sim$5			hc	9
IRAS04166	04166+2706	04 16 37.8	27 06 29	140	0.4	0.2		bip	10, 11
L1527	04368+2557	04 36 49.5	25 57 16	140	2	0.4	59[b]	hc	12, 13
RNO43-mm	05295+1247	05 29 30.6	12 47 35	400	6	0.6	33	hc	14
NGC2024/FIR5		05 39 13.0	–01 57 08	400	$>$ 10	15	20	hc,mo	15, 16, 17
NGC2024/FIR6		05 39 13.7	–01 57 30	400	$>$ 15	6	20	hc,c	15, 16, 18
HH24-mm		05 43 34.8	–00 11 49	460	5	6	25		19, 20, 21
NGC2264G	06384+0958	06 38 25.8	09 58 52	800	5			hc	22, 23, 24, 25
IRAS08076*	08076–3556	08 07 40.3	–35 56 06	450	11		74[a]	hc	5
BHR71-mm*	11590–6452	11 59 03.1	–64 52 11	200	12			hc	26, 27
VLA1623		16 23 25.0	–24 17 47	160	1	0.6	20	hc	28, 29
IRAS16293	16293–2422	16 29 21.0	–24 22 16	160	23	2	39	hc,mu	30
L483*	18148–0440	18 14 50.6	–04 40 49	200	14		49[b]	hc	12, 13
Serp/S68N		18 27 15.2	01 14 57	310			20	w	31, 32, 33, 34
Serp/FIRS1		18 27 17.3	01 13 23	310	50		35		31, 32, 33, 34
Serp/smm3		18 27 27.3	01 11 55	310	$<$ 11		$<$ 20		31, 33, 34
Serp/smm4		18 27 24.7	01 11 10	310	$<$ 11		20		31, 33, 34
L723-mm	19156+1906	19 15 42.0	19 06 55	300	3	0.6	—	mu?	35, 36
B335	19345+0727	19 34 35.1	07 27 24	250	3	0.8	30	hc	37
IRAS20050*	20050+2720	20 05 02.5	27 20 09	700	260		40	hc,mu	38, 39
S106-smm		20 25 32.4	37 12 48	600	$>$ 24	$<$10	$>$ 20		40
L1157-mm	20386+6751	20 38 39.3	67 51 36	440	11	0.5	—	hc	41, 42

* Firm classification as Class 0 source needs confirmation.

[a] Outflow characteristics: hc = highly collimated CO outflow, bip = bipolar, c = compact, mu = multiple, mo = monopolar, w = wings.

[b] Bolometric temperature in the sense of Myers & Ladd (1993).

[c] References: 1. Bachiller et al (1990), 2. Bachiller et al (1991a), 3. Bachiller et al (1995b), 4. Sandell et al (1994), 5. Hodapp & Ladd (1995), 6. Sandell et al (1991), 7. Bachiller et al (1991c), 8. Bachiller et al (1994b), 9. McCaughrean et al (1994), 10. Kenyon et al (1993), 11. Bontemps et al (1996), 12. Ladd et al (1991), 13. Myers et al (1995), 14. Zinnecker et al (1992), 15. Mezger et al (1992), 16. Mauersberger et al (1992), 17. Richer et al (1992), 18. Richer (1990), 19. Chini et al (1993), 20. Ward-Thompson et al (1995), 21. Bontemps et al (1995), 22. Margulis et al (1990), 23. Gómez et al (1994), 24. Ward-Thompson et al (1995), 25. Lada & Fich (1996), 26. Bourke & Lehtinen (1995), 27. Bourke & Lehtinen (1996), 28. André et al (1990a), 29. André et al (1993), 30. Walker et al (1986), 31. Casali et al (1993), 32. McMullin et al (1994b), 33. Hurt et al (1996), 34. White et al (1995), 35. Cabrit & André (1991), 36. Avery et al (1990), 37. Chandler et al (1990), 38. Wilking et al (1989), 39. Bachiller et al (1995a), 40. Richer et al (1993), 41. Gueth et al (1995), 42. Tafalla & Bachiller (1995).

1994), L1527 (Zhou et al 1994, Myers et al 1995), and L483 (Myers et al 1995). Note that all these are Class 0 sources and that apparently more evolved (Class I) objects exhibit no sign of infall (e.g. Zhou et al 1994).

The concept of Class 0 protostars has been introduced for low-mass YSOs, whereas high-mass counterparts of so young objects are more difficult to study because of their faster evolution and the higher confusion in the more massive and turbulent surrounding clouds. High-mass protostars could, however, have been detected as mm peaks near ultracompact HII regions (e.g. Cesaroni et al 1994), and evidence for infall has been claimed around some ultracompact HII regions (Welch et al 1987, Keto et al 1988, Rudolph et al 1990, Wilner et al 1995). We caution, however, that the interpretation in terms of infall in these objects is always complicated by the presence of strong outflows.

6. ORIGIN OF BIPOLAR MOLECULAR OUTFLOWS

6.1 *Disks*

Observations of molecular lines and of millimeter and infrared continua have provided evidence that YSOs are surrounded by circumstellar structures of about 10^2 AU and masses in the range of a few 10^{-3} to 1 $M_\odot$ (see Sargent 1996 for a recent review). Millimeter-wave continuum surveys are providing information on disk properties and on disk frequency rate in different cloud complexes (André et al 1990b; Beckwith & Sargent 1991, 1993; Reipurth et al 1993; Osterloh & Beckwith 1995). The *HST* has observed externally illuminated disks in the Orion complex and disks in absorption against the nebular background of the Orion clouds (O'Dell et al 1993, O'Dell & Wen 1994).

Disks are also necessary to explain a number of observational facts: 1. the asymmetries of the forbidden line profiles observed around YSOs, because the preferentially blueshifted profiles are assumed to result from the disk occultation of the redshifted emission (Appenzeller et al 1984, Edwards et al 1987), 2. the SEDs of the classical T Tau stars, since the typical spectral index of viscous disks explains quite accurately the IR observations (Bertout et al 1988), 3. the excess observed in the optical and UV ranges, which is responsible for the veiling of the photospheric absorption lines (Bertout 1989), and 4. the eruptions of FU Ori stars that can be understood as resulting from activity in the accretion disks (e.g. Hartmann & Kenyon 1985, Croswell et al 1987).

The physical parameters of the disks are difficult to obtain. Infrared observations provide the total spectrum of the star/disk system, and sophisticated models are necessary to extract disk properties (e.g. Bertout et al 1988). Interferometric observations at millimeter wavelengths currently provide the

needed resolution to directly observe the gas and dust emission from some disks (Sargent & Welch 1993), but these disks may be surrounded by more extended envelopes that introduce confusion in the observations. In particular, scattering of the disk radiation in the envelope can produce a far-infrared or submillimeter excess (Natta 1993), distorting the SED of the disk (Butner et al 1994). These envelopes can also bias the interpretation of mm-wave continuum emission (Terebey et al 1993).

The interpretation of molecular line observations is also complicated by the coexistence of the disk rotation with other systematic motions such as infall and outflow. Convincing cases of disks have been found in HL Tau (Sargent & Beckwith 1987, 1991), T Tau (Weintraub et al 1989), and GG Tau (Dutrey et al 1994). In the case of HL Tau, the presence of outflow motions makes it difficult to obtain accurate estimates of the disk parameters (Cabrit et al 1996). However, the structure of the circumbinary disk around GG Tau is well revealed by the 2″ angular resolution images of Dutrey et al (1994). It appears that the material within 180 AU of the binary has been cleared up, and the disk has a radius of 900 AU.

6.2 *Relationship of Jets and Disks*

There is increasing observational evidence for the existence of a close link between jets and disks around YSOs. For instance, in T Tau stars, forbidden line emission, which is thought to arise from an outflow, is only seen in objects presenting near-IR excesses attributed to disks (Edwards 1995). In addition, the intensity of the high-velocity emission seen in the [OI] 6300 Å line is correlated with the near-IR color excess (Edwards et al 1993). In younger objects, such relations are also well observed. In particular, Cabrit & André (1991) found the momentum flux of molecular outflows to be well correlated with the mass of the circumstellar YSO envelope as determined from mm-wave observations. This correlation was recently improved by Bontemps et al (1996), demonstrating that there is a good continuity from Class 0 to Class I sources (Figure 12). We finally note that the ubiquity of high-velocity outflows around YSOs is accompanied by corresponding very high frequency rates in the observations of disks. For instance, in embedded clusters, the fraction of young low-mass stars that have circumstellar disks exceeds 80% (Strom 1995, Dougados et al 1996).

The observed relationship between the properties of jets and disks suggests that disks are necessary to drive winds. Hartmann & McGregor (1982) showed that purely stellar winds could not explain the observed mass-loss rates in typical T Tau stars, since this would require the stars to rotate near to breakup, in contrast to the observations showing T Tau stars rotating an order of magnitude slower than breakup velocities (Vogel & Kuhi 1981, Bouvier et al 1986). The formation of disks provides a powerful mechanism to store the angular momentum during

the YSO evolution, offering a natural explanation for the slow T Tau rotation velocities. On the other hand, the neutral species (Na, HI, CO) observed at very high velocities around some YSOs suggest that the wind has a significant neutral component, supporting the idea that the wind arises from the disk, and not from the hot stellar surface (Königl & Ruden 1993).

In summary, accretion disks appear as the reservoir of momentum and energy that can potentially account for the enormous mechanical power observed in bipolar molecular outflows. In order to understand how the momentum is transferred from the disk to the wind, a series of theoretical models have been constructed. These are discussed in the next subsection.

6.3 *Models for the Wind Origin*

Purely hydrodynamical models were first constructed to explain the origin of bipolar outflows. In such models the wind was collimated externally by the

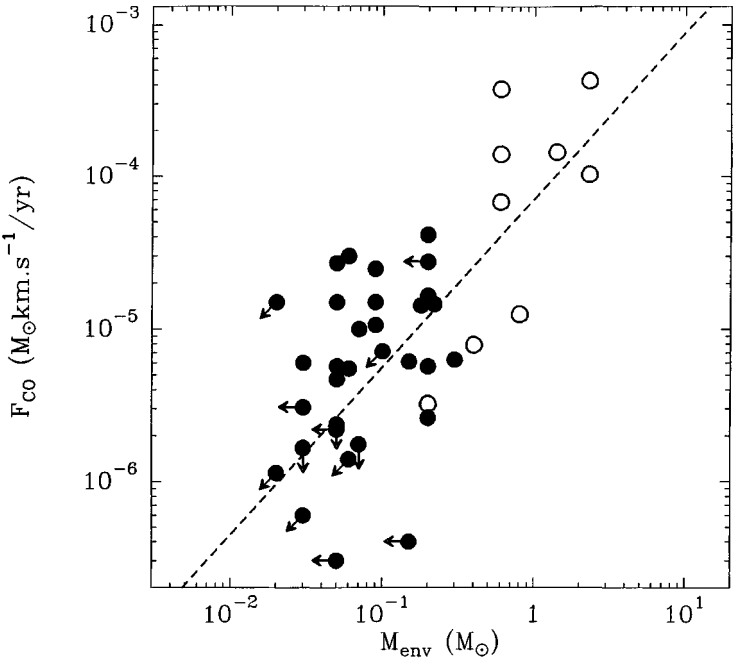

Figure 12 Momentum flux in the CO outflow vs circumstellar envelope mass for a sample of Class 0 (*open circles*) and Class I (*filled circles*) YSOs. The most powerful outflows emanate from the youngest objects with most massive envelopes. The dashed line is a fit to the observed correlation. (From Bontemps et al 1996.)

ambient medium. Barral & Cantó (1981) first proposed that an isotropic wind could be collimated by the thermal pressure from a surrounding large-scale flattened structure or disk. In fact, the wind could be collimated by the formation of de Laval nozzles when it expands through the decreasing density of the core. Such purely hydrodynamical models present the serious drawback that the jet acceleration depends strongly on the shape of the nozzle generated by the external pressure, i.e. the structure of the external medium critically determines the jet properties. Furthermore, as Königl (1982) concluded, a magnetic field is necessary to create the initial anisotropy, determining for instance the orientation of the protostellar disk by means of magnetic braking (Mouschovias & Paleologou 1980), which will eventually determine the jet orientation.

Magnetic fields seem also necessary to launch the wind. As De Campli (1981) pointed out, thermal pressure alone cannot generate the observed outflows, because the temperatures implied at the base of the flow would be very high, and the radiative losses (e.g. by X rays) would be several orders of magnitude higher than the stellar luminosity (Königl & Ruden 1993). However, a magnetic field coupled to the rotating disk surrounding the YSO provides a potentially powerful engine to explain the production of jets. It thus follows that the most suitable models for the origin of protostellar jets are those of magnetohydrodynamical (MHD) disk-driven winds. These models can be divided into two categories, depending on whether the jet arises at the disk surface or at the star/disk boundary layer.

6.3.1 DISK-DRIVEN WINDS The model of Blandford & Payne (1982) for extragalactic jets was soon applied to the case of the YSO jets (Pudritz & Norman 1983, 1986; Pudritz 1985; Königl 1989). In these models accretion and ejection are interdependent processes, and the wind is centrifugally driven by the poloidal magnetic fields threading the disk. Lovelace et al (1991, 1993) have tried to simplify the problem by averaging the different physical variables over the cross section of the jet at a given distance from the equatorial plane. Further refinements of MHD analytical models have been recently done by Appl & Camenzind (1992), Pudritz et al (1991), Pelletier & Pudritz (1992), Contopoulos & Lovelace (1994), and Rosso & Pelletier (1994). Numerical simulations have been carried out by Uchida & Shibata (1985) and Shibata & Uchida (1986). Most of these models do not consider the detailed structure of the disk at the base of the jet. However, as discussed above, observations suggest that the structures of the jet and disk are intimately related, so that accretion and ejection should be modeled together. Königl (1989) was the first to consider the disk structure with realistic magnetic fields. Wardle & Königl (1993) refined this model for the disk structure. Recent self-consistent models

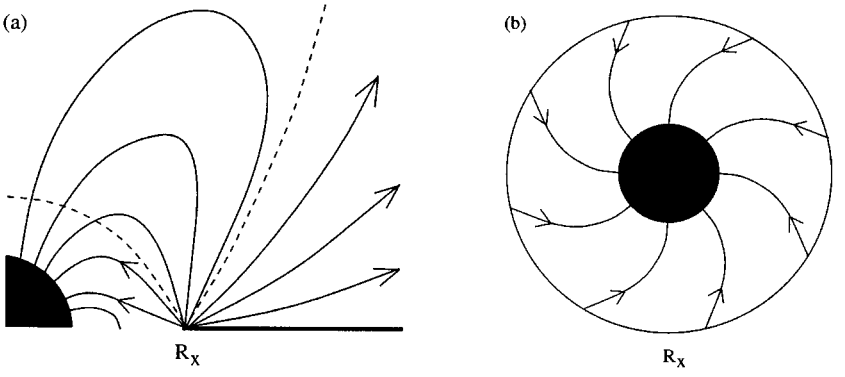

Figure 13 Schematic views of the (*a*) meridional plane and (*b*) equatorial plane of the configuration modeled by Shu et al (1994a,b) for the origin of bipolar outflows. The circumstellar disk is truncated at a distance R_X from the star. Both energetic outflows and funnel flows emerge from the disk truncation region. Gas accreting from the disk onto the star in a funnel flow drags the stellar field into a trailing spiral pattern. (From Najita 1995.)

of magnetized accretion-ejection structures have been developed by Ferreira & Pelletier (1993a,b, 1995).

Some problems of the disk-wind models remain poorly understood. The required magnetic field in the disk has to be maintained by a turbulent dynamo process, but the fields generated by the dynamo process are expected to be too weak (Stepinski & Levy 1990, 1991). Also, as emphasized by Shu (1995), the external magnetic fields retained in viscous disks are probably insufficient to launch the wind, owing to the likely low ionization of the disks.

6.3.2 BOUNDARY LAYER–DRIVEN WINDS In the boundary layer between the accretion disk and the star the rotational velocity of the disk is regulated to the star rotational velocity. This region is expected to be an important reservoir of energy where jets could potentially be efficiently formed. Torbett (1984) proposed that the shock developed by the effect of the accretion combined with the thermal instabilities were responsible for the generation of jets. This model, however, presents the same problems as thermal stellar winds (De Campli 1981). Pringle (1989) suggested that a strong toroidal magnetic field could be produced at the boundary layer by a dynamo effect, but the details of the ejection process were not modeled. Other models that place the origin of the jet at the boundary layer have been proposed by Camenzind (1990) and Bertout & Regev (1992).

The most popular model of this category is that of the X-celerator. This model assumed initially (Shu et al 1988) that the jet was generated at the region of the

stellar equator where centrifugal and gravitational forces are compensated (the X-point). The YSO was assumed to have a strong magnetic field and was able to continue accreting by ejecting a strong outflow at a significant fraction of the infall rate. Since the mass-loss happens on the equatorial plane, the optical jets are produced by the expansion of the flow toward the rotational poles. The main difficulty of this model is that the star needs to rotate at breakup at its equator, while actual T Tauri stars are known to rotate at about a tenth of this velocity (Bouvier et al 1986). Recently, the X-celerator model has been modified (Shu et al 1994a,b; Najita & Shu 1994; Ostriker & Shu 1995) to allow for the star rotating below breakup. Following a suggestion by Königl (1991), it is assumed that the stellar magnetic field is strong enough to truncate the disk at a radius R_X from the star (Figure 13). The rapid rotation of the material in a small region around this radius seems able to drive a funnel inflow into the star together with a X-type outflow.

7. CONCLUSION

Bipolar outflows are ubiquitous around young stars and involve amounts of energy similar to those involved in the accretion processes. Thus, outflows are a dominant ingredient in the formation of stars. Outflows probably limit the mass of the star/disk system under formation and are indispensable for transporting away the excess angular momentum of accretion disks. Outflows seem able to perturb the dense gas within the cores where stars are born, and they could determine the dense core evolution after the first stellar generation. The youngest stellar objects presently known (the so-called Class 0 protostars) are sources of energetic outflows, implying that outflow and infall motions happen simultaneously and are closely linked from the very beginning stages of the star formation process. The idea of a new star forming from relatively simple hydrodynamic infall is giving way to a picture in which magnetic fields play a crucial role and stars are born through the formation of complex engines of accretion/ejection. The next generation of millimeter-wave interferometers will be decisive in elucidating the structure of such engines and will probably reveal unexpected phenomena related to the origin of outflows. It seems inevitable that future theories of star formation will have to take into account, together with the structure of the protostar and its surrounding accretion disk, the processes of infall and outflow in a unified manner.

ACKNOWLEDGMENTS

It is a pleasure to acknowledge Drs. André, Cabrit, Cernicharo, Dutrey, Eislöffel, Fuente, Gómez-González, Gueth, Guilloteau, Mardones, Martín-Pintado, Myers,

Reipurth, Richer, Tafalla, Pérez-Gutiérrez, and Planesas for interesting discussions and fruitful collaborative work on outflows during the past years. Drs. Eislöffel, Reipurth, and Tafalla gave me many comments and suggestions that helped to improve the manuscript. I also thank Drs. Bontemps and McCaughrean for providing figures and the numerous colleagues who provided manuscripts in advance of publication. A part of this article was written while I was guest professor at the Observatoire de Grenoble (France), where I enjoyed a friendly and stimulating atmosphere. Funding support from Spanish DGICYT (through grant PB93–48) is gratefully acknowledged.

Literature Cited

Adams FC, Lada CJ, Shu FH. 1987. *Ap. J.* 312:788–806
Allamandola LJ, Sandford SA, Tielens AGGM, Herbst T. 1992. *Ap. J.* 399:134–46
Allen DA, Burton MG. 1993. *Nature* 363:54–56
André P. 1994. In *The Cold Universe*, ed. T Montmerle, CJ Lada, IF Mirabel, J Trân Thanh Vân, pp. 179–92. Gif-sur-Yvette, France: Frontières.
André P. 1995. In *Circumstellar Matter*, ed. G Watt, P Williams, pp. 29–42. Dordrecht: Kluwer.
André P, Martín-Pintado J, Despois D, Montmerle T. 1990a. *Astron. Astrophys.* 236:180–92
André P, Montmerle T. 1994. *Ap. J.* 420:837–62
André P, Montmerle T, Feigelson ED, Steppe H. 1990b. *Astron. Astrophys.* 240:321–30
André P, Ward-Thompson D, Barsony M. 1993. *Ap. J.* 406:122–41
Appenzeller I, Jankovics I, Östreicher R. 1984. *Astron. Astrophys.* 141:108–15
Appenzeller I, Mundt R. 1989. *Astron. Astrophys. Rev.* 1:191–234
Appl S, Camenzind M. 1992. *Astron. Astrophys.* 256:354–70
Avery LW, Hayashi SS, White GJ. 1990. *Ap. J.* 357:524–30
Bachiller R, André P, Cabrit S. 1991a. *Astron. Astrophys.* 241:L43–46
Bachiller R, Cernicharo J. 1990. *Astron. Astrophys.* 239:276–86
Bachiller R, Cernicharo J, Martín-Pintado J, Tafalla M, Lazareff B. 1990. *Astron. Astrophys.* 231:174–86
Bachiller R, Fuente A, Tafalla M. 1995a. *Ap. J. Lett.* 445:L51–54
Bachiller R, Gómez-González J. 1992. *Astron. Astrophys. Rev.* 3:257–87
Bachiller R, Guilloteau S, Dutrey A, Planesas P, Martín-Pintado J. 1995b. *Astron. Astrophys.* 299:857–68
Bachiller R, Guilloteau S, Kahane C. 1987. *Astron. Astrophys.* 173:324–36
Bachiller R, Liechti S, Walmsley CM, Colomer F. 1995c. *Astron. Astrophys.* 295:L51–54
Bachiller R, Martín-Pintado J, Fuente A. 1991b. *Astron. Astrophys.* 243:L21–24
Bachiller R, Martín-Pintado J, Fuente A. 1993. *Ap. J. Lett.* 417:L45–48
Bachiller R, Martín-Pintado J, Planesas P. 1991c. *Astron. Astrophys.* 251:639–48
Bachiller R, Tafalla M, Cernicharo J. 1994a. *Ap. J. Lett.* 425:L93–96
Bachiller R, Terebey S, Jarrett T, Martín-Pintado J, Beichman CA, van Buren D. 1994b. *Ap. J.* 437:296–304
Bally J, Castets A, Duvert D. 1994. *Ap. J.* 423:310–19
Bally J, Devine D. 1994. *Ap. J. Lett.* 428:L65–68
Bally J, Devine D, Fesen RA. 1995. *Ap. J.* 454:345–60
Bally J, Devine D, Hereld M, Rauscher BJ. 1993a. *Ap. J. Lett.* 418:L75–78
Bally J, Lada CJ. 1983. *Ap. J.* 265:824–47
Bally J, Lada CJ, Lane, AP. 1993b. *Ap. J.* 418:322–27
Bally J, Lane AP. 1990. In *Astrophysics with Infrared Arrays*, ed. R Elston, p. 273. San Francisco: Astron. Soc. Pac.
Bally J, Stark AA. 1983. *Ap. J. Lett.* 266:L61–64
Barral P, Cantó J. 1981. *Rev. Mex. Astron. Astrofis.* 5:101–8

Barsony M. 1995. In *Clouds, Cores, and Low Mass Stars*, ed. DP Clemens, R Barvainis, pp. 197–206. San Francisco: Astron. Soc. Pac.
Beckwith SVW, Sargent AI. 1991. *Ap. J.* 381:250–58
Beckwith SVW, Sargent AI. 1993. *Ap. J.* 402:280–91
Benson PC, Myers PC. 1989. *Ap. J. Suppl.* 71:89–108
Bertout C. 1989. *Annu. Rev. Astron. Astrophys.* 27:351–95
Bertout C, Basri G, Bouvier J. 1988. *Ap. J.* 330:350–73
Bertout C, Regev O. 1992. *Ap. J. Lett.* 399:L163–66
Bieging JH, Cohen M. 1985. *Ap. J. Lett.* 289:L5–8
Bieging JH, Cohen M, Schwartz PR. 1984. *Ap. J.* 282:699–708
Biro S, Raga AC. 1994. *Ap. J.* 434:221–31
Blake GA, Sandell G, van Dishoeck EF, Groesbeck TD, Mundy LG. 1995. *Ap. J.* 441:689–701
Blake GA, Sutton EC, Masson CR, Phillips TG. 1987. *Ap. J.* 315:621–45
Blake GA, van Dishoeck EF, Jansen DJ, Groesbeck TD, Mundy LG. 1994. *Ap. J.* 428:680–92
Blandford RD, Payne DG. 1982. *MNRAS* 199:883–903
Blondin JM, Fryxell BA, Königl A. 1990. *Ap. J.* 360:370–86
Bontemps S, André P, Terebey S, Cabrit S. 1996. *Astron. Astrophys.* In Press
Bontemps S, André P, Ward-Thompson D. 1995. *Astron. Astrophys.* 297:98–102
Bourke TL, Lehtinen KK. 1995. In *CO: Twenty-Five Years of Millimeter-Wave Spectroscopy. IAU Symp. 170.* In press
Bourke TL, Lehtinen KK. 1996. Preprint
Bouvier J, Bertout C, Benz W, Mayor M. 1986. *Astron. Astrophys.* 165:110–19
Bührke Th, Mundt R, Ray TP. 1988. *Astron. Astrophys.* 200:99–119
Butner HM, Natta A, Evans NJ II. 1994. *Ap. J.* 420:326–35
Cabrit S. 1993. In *Stellar Jets and Bipolar Outflows*, ed. L Errico, A Vittone, pp. 1–14. Dordrecht: Kluwer
Cabrit S, André P. 1991. *Ap. J. Lett.* 379:L25–28
Cabrit S, Bertout C. 1986. *Ap. J.* 307:313–23
Cabrit S, Bertout C. 1990. *Ap. J.* 348:530–41
Cabrit S, Bertout C. 1992. *Astron. Astrophys.* 261:274–84
Cabrit S, Edwards S, Strom SE, Strom KM. 1990. *Ap. J.* 354:687–700
Cabrit S, Goldsmith PF, Snell RL. 1988. *Ap. J.* 334:196–208
Cabrit S, Guilloteau S, André P, Bertout C, Montmerle T, Schuster K. 1996. *Astron. Astrophys.* 305:527–40
Camenzind M. 1990. *Rev. Mod. Astron.* 3:234–65
Campbell B, Person SE, Strom SE, Grasdalen GL. 1988. *Astron. J.* 95:1173–84
Cantó J, Raga A. 1991. *Ap. J.* 372:646–58
Carr JS, Harvey PM, Lester DF. 1987. *Ap. J. Lett.* 321:L71–74
Casali MM, Eiroa C. 1995. *Rev. Mex. Astron. Astrof. (Ser. Conf.)* 1:303–7
Casali MM, Eiroa C, Duncan WD. 1993. *Astron. Astrophys.* 275:195–200
Cernicharo J, Bachiller R, Duvert G, González-Alfonso E, Gómez-González J. 1992. *Astron. Astrophys.* 261:589–601
Cernicharo J, Neri R, Reipurth B, Bachiller R. 1996. Preprint
Cernicharo J, Reipurth B. 1996. Preprint
Cesaroni R, Olmi L, Walmsley CM, Churchwell E, Hofner P. 1994. *Ap. J. Lett.* 435:L137–41
Chandler CJ, Gear WK, Sandell G, Hayashi S, Duncan WD, et al. 1990. *MNRAS* 243:330–35
Chen H, Myers PC, Ladd EF, Wood DO. 1995. *Ap. J.* 445:377–92
Chernin LM, Masson CR. 1991. *Ap. J. Lett.* 382:L93–96
Chernin LM, Masson CR. 1995a. *Ap. J.* 443:181–86
Chernin LM, Masson CR. 1995b. *Ap. J.* 455:182–89
Chernin LM, Masson CR, Fuller G. 1994a. *Ap. J.* 436:741–48
Chernin LM, Masson CR, Gouveia Dal Pino EM, Benz W. 1994b. *Ap. J.* 426:204–14
Chini R, Krügel E, Haslam CGT, Kreysa E, Lemke R, et al. 1993. *Astron. Astrophys.* 272:L5– 8
Clark FO, Laurejis RJ. 1986. *Astron. Astrophys.* 154:L26–29
Cohen M, Bieging JH, Schwartz PR. 1982. *Ap. J.* 253:707–15
Contopoulos J, Lovelace RVE. 1994. *Ap. J.* 429:139–52
Croswell K, Hartmann L, Avret EH. 1987. *Ap. J.* 312:227–42
Cudworth KM, Herbig GH. 1979. *Astron. J.* 84:548–51
Curiel S, Rodríguez LF, Moran JM, Cantó J. 1993. *Ap. J.* 415:191–203
Davis CJ, Dent WRF, Matthews HE, Aspin C, Lightfoot JF. 1994a. *MNRAS* 266:933–44
Davis CJ, Eislöffel J. 1995. *Astron. Astrophys.* 300:851–69
Davis CJ, Eislöffel J, Ray TP. 1994b. *Ap. J. Lett.* 426:L93–95
Davis CJ, Mundt R, Eislöffel J. 1994c. *Ap. J. Lett.* 437:L55–58
Davis CJ, Mundt R, Eislöffel J, Ray TP. 1995. *Astron. J.* 110:766–75

De Campli WM. 1981. *Ap. J.* 244:124–46
Dent WRF, Matthews HE, Walther DM. 1995. *MNRAS* 277:193–209
De Young DS. 1986. *Ap. J.* 307:62–72
Dopita MA, Schwartz R, Evans I. 1982. *Ap. J.* 263:L73–76
Dougados C, Carpenter J, Meyer M, Strom SE. 1996. Preprint
Draine BT, Roberge WG, Dalgarno A. 1983. *Ap. J.* 264:485–507
Dutrey A, Guilloteau S, Bachiller R. 1996. Preprint
Dutrey A, Guilloteau S, Simon M. 1994. *Astron. Astrophys.* 286:149–59
Dyson JE. 1984. *Astrophys. Space Sci.* 106:181–97
Edwards S. 1995. *Rev. Mex. Astron. Astrof. (Ser. Conf.)* 1:309–16
Edwards S, Cabrit S, Strom SE, Heyer I, Strom KM, Andrson E. 1987. *Ap. J.* 321:473–95
Edwards S, Ray T, Mundt R. 1993. In *Protostars and Planets III*, ed. EH Levy, JI Lunine, pp. 567–602. Tucson: Univ. Ariz. Press
Edwards S, Snell RL. 1982. *Ap. J.* 261:151–60
Edwards S, Snell RL. 1983. *Ap. J.* 270:605–19
Edwards S, Snell RL. 1984. *Ap. J.* 281:237–49
Edwards S, Strom SE, Snell RL, Jarrett TH, Beichman CA, Strom KM. 1986. *Ap. J. Lett.* 307:L65–68
Eislöffel J, Davis CJ, Ray TP, Mundt R. 1994. *Ap. J. Lett.* 422:L91–93
Eislöffel J, Mundt R. 1994. *Astron. Astrophys.* 284:530–44
Ferreira J, Pelletier G. 1993a. *Astron. Astrophys.* 276:625–36
Ferreira J, Pelletier G. 1993b. *Astron. Astrophys.* 276:637–47
Ferreira J, Pelletier G. 1995. *Astron. Astrophys.* 295:807–32
Fukui Y, Iwata T, Mizuno A, Bally J, Lane AP. 1993. In *Protostars and Planets III*, ed. EH Levy, JI Lunine, pp. 603–39. Tucson: Univ. Ariz. Press
Garden RP, Hayashi M, Gatley I, Hasegawa T, Kaifu N. 1991. *Ap. J.* 374:540–54
Giovanardi C, Lizano S, Natta A, Evans NJ II, Heiles C. 1992. *Ap. J.* 397:214–24
Glassgold AE, Mamon GA, Huggins PJ. 1989. *Ap. J. Lett.* 336:L29–32
Glassgold AE, Mamon GA, Huggins PJ. 1991. *Ap. J.* 373:254–65
Goldsmith PF, Snell RL, Hemeon-Heyer M, Langer WD. 1984. *Ap. J.* 286:599–608
Gómez JF, Curiel S, Torrelles JM, Rodríguez LF, Anglada G, Girart JM. 1994. *Ap. J.* 436:749–53
Gouveia Dal Pino EM, Benz W. 1993. *Ap. J.* 410:686–95
Gredel R, Reipurth B. 1993. *Ap. J. Lett.* 407:L29–32
Gredel R, Reipurth B. 1994. *Astron. Astrophys.* 289:L19–22
Gueth F, Guilloteau S, Bachiller R. 1996. *Astron. Astrophys.* In press
Guilloteau S, Bachiller R, Lucas R, Fuente A. 1992. *Astron. Astrophys.* 265:L49–52
Gwinn CR, Moran JM, Reid MJ. 1992. *Ap. J.* 393:149–64
Haro G. 1952. *Ap. J.* 115:572–73
Hartigan P, Morse JA, Heathcote S, Cecil G. 1993. *Ap. J. Lett.* 414:L121–24
Hartigan P, Raymond PC. 1993. *Ap. J.* 409:705–19
Hartmann L, Kenyon SJ. 1985. *Ap. J.* 299:462–78
Hartmann L, McGregor KB. 1982. *Ap. J.* 259:180–92
Henriksen RN, Ptuskin VS, Mirabel IF. 1991. *Astron. Astrophys.* 248:221–26
Herbig G. 1951. *Ap. J.* 113:697–99
Herbig G. 1962. *Adv. Astron. Astrophys.* 1:47–103
Hirth GA, Mundt R, Solf J. 1994a. *Astron. Astrophys.* 285:929–42
Hirth GA, Mundt R, Solf J, Ray TP. 1994b. *Ap. J. Lett.* 427:L99–102
Hodapp KW. 1994. *Ap. J. Suppl.* 94:615–49
Hodapp KW, Deane J. 1993. *Ap. J. Suppl.* 88:119–35
Hodapp KW, Ladd EF. 1995. *Ap. J.* 453:715–20
Hurt RL, Barsony M, Wootten A. 1996. *Ap. J.* 456:686–95
Iglesias ER, Silk J. 1978. *Ap. J.* 226:851–57
Iwata T, Fukui Y, Ogawa H. 1988. *Ap. J.* 325:372–81
Kenyon SJ, Calvet N, Hartmann L. 1993. *Ap. J.* 414:676–94
Keto ER, Ho PTP, Haschick AD. 1988. *Ap. J.* 324:920–30
Kitamura Y, Kawabe R, Yamashita T, Hayashi M. 1990. *Ap. J.* 363:180–91
Königl A. 1982. *Ap. J.* 261:115–34
Königl A. 1989. *Ap. J.* 342:208–23
Königl A. 1991. *Ap. J. Lett.* 370:L39–43
Königl A, Ruden SP. 1993. In *Protostars and Planets III*, ed. EH Levy, JI Lunine, pp. 641–87. Tucson: Univ. Ariz. Press
Kuhi LV. 1964. *Ap. J.* 140:1409–33
Kwan J, Scoville N. 1976. *Ap. J. Lett.* 210:L39–42
Kwan J, Tademaru E. 1988. *Ap. J. Lett.* 332:L41–44
Lada CJ. 1985. *Annu. Rev. Astron. Astrophys.* 23:267–317
Lada CJ. 1991. In *The Physics of Star Formation and Early Evolution*, ed. CJ Lada, ND Kylafis, pp. 329–63. Kluwer: Dordrecht
Lada CJ, Fich M. 1996. *Ap. J.* 459:638–52
Lada CJ, Wilking BA. 1984. *Ap. J.* 287:610–21
Ladd EF, Adams FC, Casey S, Davidson JA,

Fuller GA, et al. 1991. *Ap. J.* 366:203–20
Lane AP. 1989. In *ESO Workshop on Low Mass Star Formation and Pre-Main Sequence Objects*, ed. B Reipurth, pp. 331–48. Garching: ESO
Lizano S, Giovanardi C. 1995. *Ap. J.* 447:742–51
Lizano S, Heiles C, Rodríguez LF, Koo BC, Shu FH, et al. 1988. *Ap. J.* 328:763–76
Lovelace RVE, Berk HL, Contopoulos J. 1991. *Ap. J.* 376:696–705
Lovelace RVE, Romanova MM, Contopoulos J. 1993. *Ap. J.* 403:158–63
Mac Low MM, Elitzur M. 1992. *Ap. J. Lett.* 393:L33–36
Mac Low MM, Elitzur M, Stone JM, Königl A. 1994. *Ap. J.* 427:914–18
Margulis M, Lada CJ. 1985. *Ap. J.* 299:925–38
Margulis M, Lada CJ, Hasegawa T, Hayashi SS, Hayashi M, et al. 1990. *Ap. J.* 352:615–24
Martí J, Rodríguez LF, Reipurth B. 1993. *Ap. J.* 416:208–17
Martí J, Rodríguez LF, Reipurth B. 1995. *Ap. J.* 449:184–87
Martín-Pintado J, Bachiller R, Fuente A. 1992. *Astron. Astrophys.* 254:315–26
Masson CR, Chernin LM. 1992. *Ap. J. Lett.* 387:L47–50
Masson CR, Chernin LM. 1993. *Ap. J.* 414:230–41
Masson CR, Mundy LG, Keene J. 1990. *Ap. J. Lett.* 357:L25–28
Mathieu RD. 1994. *Annu. Rev. Astron. Astrophys.* 32:465–530
Mauersberger R, Wilson TL, Mezger PG, Gaume R, Johnston KJ. 1992. *Astron. Astrophys.* 256:640–51
McCaughrean MJ, Rayner JT, Zinnecker H. 1994. *Ap. J. Lett.* 436:L189–93
McMullin JP, Mundy LG, Blake GA. 1994a. *Ap. J.* 437:305–16
McMullin JP, Mundy LG, Wilking BA, Hetzel T, Blake GA. 1994b. *Ap. J.* 424:222–36
Menten KM, Walmsley CM. 1985. *Ap. J.* 146:369–74
Meyers-Rice BA, Lada CJ. 1991. *Ap. J.* 368:445–62
Mezger PG, Sievers AW, Haslam CGT, Kreysa E, Lemke R, et al. 1992. *Astron. Astrophys.* 256:631–39
Millar TJ, Herbst E, Charnley SB. 1991. *Ap. J.* 369:147–56
Mitchell GF, Maillard JP, Hasegawa TI. 1991. *Ap. J.* 371:342–56
Morse JA, Hartigan P, Cecil G, Raymond JC, Heathcote S. 1992. *Ap. J.* 399:231–45
Mouschovias T, Paleologou EV. 1980. *Ap. J.* 237:877–99
Mundt R. 1984. *Ap. J.* 280:749–70
Mundt R, Brugel EW, Bührke T. 1987. *Ap. J.* 319:275–303
Mundt R, Fried JW. 1983. *Ap. J. Lett.* 274:L83–86
Mundt R, Stocke J, Strom SE, Strom KM, Anderson ER. 1985. *Ap. J. Lett.* 297:L41–44
Myers PC, Bachiller RB, Caselli P, Fuller GA, Mardones D, et al. 1995. *Ap. J. Lett.* 449:L65–68
Myers PC, Fuller GA, Mathieu RD, Beichman CA, Benson PJ, et al. 1987. *Ap. J.* 319:340–57
Myers PC, Heyer M, Snell RL, Goldsmith PF. 1988. *Ap. J.* 324:907–19
Myers PC, Ladd EF. 1993. *Ap. J. Lett.* 413:L47–50
Najita JR. 1995. *Rev. Mex. Astron. Astrof. (Ser. Conf.)* 1:293–301
Najita JR, Shu FH. 1994. *Ap. J.* 429:808–25
Natta A. 1993. *Ap. J.* 412:761–70
Natta A, Giovanardi C. 1990. *Ap. J.* 356:646–61
Natta A, Giovanardi C, Palla F, Evans NJ Jr. 1988. *Ap. J.* 327:817–21
Neckel T, Staude J. 1987. *Ap. J. Lett.* 322:L27–30
Neufeld DA, Dalgarno A. 1989. *Ap. J.* 340:869–93
O'Dell CR, Wen Z. 1994. *Ap. J.* 436:194–202
O'Dell CR, Wen Z, Hu X. 1993. *Ap. J.* 410:696–700
Olberg M, Reipurth B, Booth R. 1992. *Astron. Astrophys.* 259:252–56
Osterbrock DE. 1958. *Publ. Astron. Soc. Pac.* 70:399–403
Osterloh M, Beckwith SVW. 1995. *Ap. J.* 439:288–302
Ostriker EC, Shu FH. 1995. *Ap. J.* 447:813–28
Parker ND, Padman R, Scott PF. 1991. *MNRAS* 252:442–61
Pelletier G, Pudritz RE. 1992. *Ap. J.* 394:117–38
Pineau des Forêts G, Roueff E, Schilke P, Flower DR. 1993. *MNRAS* 262:915–28
Plambeck RL, Snell RL, Loren RB. 1983. *Ap. J.* 266:321–30
Plambeck RL, Wright MCH. 1987. *Ap. J. Lett.* 317:L101–5
Plambeck RL, Wright MCH, Welch WJ, Bieging JH, Baud B, et al. 1982. *Ap. J.* 259:617–24
Pravdo SH, Rodríguez LF, Curiel S, Cantó J, Torrelles JM, et al. 1985. *Ap. J. Lett.* 293:L35–38
Pringle JE. 1989. *MNRAS* 236:107–15
Pudritz RE. 1985. *Ap. J.* 293:216–29
Pudritz RE, Norman CA. 1983. *Ap. J.* 274:677–97
Pudritz RE, Norman CA. 1986. *Ap. J.* 301:571–86
Pudritz RE, Pelletier G, Gómez de Castro AI. 1991. In *The Physics of Star Formation and Early Evolution*, ed. CJ Lada, ND Kylafis,

pp. 539–64. Kluwer: Dordrecht
Raga AC. 1988. *Ap. J.* 335:820–28
Raga AC. 1991. *Astron. J.* 101:1472–75
Raga AC, Cabrit S. 1993. *Astron. Astrophys.* 278:267–78
Raga AC, Cantó J, Biro S. 1993a. *MNRAS* 260:163–70
Raga AC, Cantó J, Calvet N, Rodríguez LF, Torrelles JM. 1993b. *Astron. Astrophys.* 276:539–48
Raga AC, Kofman L. 1992. *Ap. J.* 386:222–28
Ray TP. 1993. In *Stellar Jets and Bipolar Outflows*, ed. L Errico, A Vittone, pp 241–56. Dordrecht: Kluwer
Reipurth B. 1989. *Nature* 340:42–44
Reipurth B. 1991. In *The Physics of Star Formation and Early Evolution*, ed. CJ Lada, ND Kylafis, pp. 497–538. Kluwer: Dordrecht
Reipurth B, Bachiller R. 1996. In *CO:Twenty-Five Years of Millimeter-Wave Spectroscopy. IAU Symp. 170.* In press
Reipurth B, Bally J, Graham JA, Lane AP, Zealey WJ. 1986. *Astron. Astrophys.* 164:51–66
Reipurth B, Cernicharo C. 1995. *Rev. Mex. Astron. Astrof. (Ser. Conf.)* 1:43–58
Reipurth B, Chini R, Krügel E, Kreysa E, Sievers A. 1993. *Astron. Astrophys.* 273:221–38
Reipurth B, Graham JA. 1988. *Astron. Astrophys.* 202:219–39
Reipurth B, Heathcote S. 1991. *Astron. Astrophys.* 246:511–34
Reipurth B, Heathcote S. 1992. *Astron. Astrophys.* 257:693–700
Reynolds SP. 1986. *Ap. J.* 304:713–20
Richer JS. 1990. *MNRAS* 245:24p–27p
Richer JS, Hills RE, Padman R. 1992. *MNRAS* 254:525–38
Richer JS, Hills RE, Padman R, Russell APG. 1989. *MNRAS* 241:231–46
Richer JS, Padman R, Ward-Thompson D, Hills RE, Harris AI. 1993. *MNRAS* 262:839–54
Rodríguez LF. 1995. *Rev. Mex. Astron. Astrof. (Ser. Conf.)* 1:1–10
Rodríguez LF, Ho PTP, Moran JM. 1980. *Ap. J. Lett.* 240:L149–52
Rodríguez LF, Lizano S, Cantó J, Escalante V, Mirabel IF. 1990. *Ap. J.* 365:261–68
Rodríguez LF, Reipurth B. 1989. *Rev. Mex. Astron. Astrof.* 17:59–63
Rodríguez-Franco A. 1995. *Condiciones físicas y químicas en la nube molecular Orión A.* PhD thesis. Univ. Complutense, Madrid
Rosso F, Pelletier G. 1994. *Astron. Astrophys.* 287:325–37
Rudolph A, Welch WJ, Palmer P, Dubrulle B. 1990. *Ap. J.* 363:528–46
Ruiz A, Alonso JL, Mirabel IF. 1992. *Ap. J. Lett.* 394:L57–60
Russell APG, Bally J, Padman R, Hills RE. 1992. *Ap. J.* 387:219–28
Sandell G, Aspin C, Duncan WD, Russell APG, Robson IE. 1991. *Ap. J. Lett.* 376:L17–20
Sandell G, Knee LBG, Aspin C, Robson IE, Russell APG. 1994. *Astron. Astrophys.* 285:L1–4
Sargent AI. 1996. In *Disks and Outflows around Young Stars*, ed. SVW Beckwith, A Natta, J Staude. Berlin: Springer-Verlag. In press
Sargent AI, Beckwith SVW. 1987. *Ap. J.* 323:294–305
Sargent AI, Beckwith SVW. 1991. *Ap. J. Lett.* 382:L31–34
Sargent AI, Welch WJ. 1993. *Annu. Rev. Astron. Astrophys.* 31:297–343
Schmid-Burgk J, Güsten R, Mauersberger R, Schulz A, Wilson TL. 1990. *Ap. J. Lett.* 362:L25–28
Schmid-Burgk J, Muders D. 1995. In *Stellar and Circumstellar Astrophysics*, ed. G Wallerstein, A Noriega-Crespo. San Francisco: ASP Conf. Ser.
Schwartz RD. 1975. *Ap. J.* 195:631–42
Schwartz RD, Williams PM, Cohen M, Jennings DG. 1988. *Ap. J.* 334:99–102
Scoville NZ, Kwan J. 1976. *Ap. J.* 206:718–27
Shibata K, Uchida Y. 1986. *Publ. Astron. Soc. Jpn.* 38:631–60
Shu FH. 1995. *Rev. Mex. Astron. Astrof. (Ser. Conf.)* 1:375–86
Shu FH, Adams FC, Lizano S. 1987. *Annu. Rev. Astron. Astrophys.* 25:23–81
Shu FH, Lizano S, Ruden SP, Najita J. 1988. *Ap. J. Lett.* 328:L19–23
Shu FH, Najita J, Ostriker E, Wilkin F, Ruden S, Lizano S. 1994a. *Ap. J.* 429:781–96
Shu FH, Najita J, Ruden S, Lizano S. 1994b. *Ap. J.* 429:797–807
Shu FH, Ruden SP, Lada CJ, Lizano S. 1991. *Ap. J. Lett.* 370:L31–34
Shull JM, Beckwith S. 1982. *Annu. Rev. Astron. Astrophys.* 20:163–90
Smith MD. 1994. *MNRAS* 266:238–46
Snell RL, Loren RB, Plambeck RL. 1980. *Ap. J. Lett.* 239:L17–20
Snell RL, Scoville NZ, Sanders DB, Erickson NR. 1984. *Ap. J.* 284:176–93
Stahler SW. 1993. In *Astrophysical Jets*, ed. M Livio, C O'Dea, D Burgarella, p. 183–209. Cambridge: Cambridge Univ. Press
Stahler SW. 1994. *Ap. J.* 422:616–20
Stapelfeldt KR, Beichman CA, Hester JJ, Scoville NZ, Gautier TN. 1991. *Ap. J.* 371:226–36
Stepinski TF, Levy EH. 1990. *Ap. J.* 350:819–26
Stepinski TF, Levy EH. 1991. *Ap. J.* 379:343–55
Stone JM, Norman ML. 1994. *Ap. J.* 420:237–46
Strom SE. 1995. *Rev. Mex. Astron. Astrof. (Ser. Conf.)* 1:317–28
Tafalla M, Bachiller R. 1995. *Ap. J. Lett.*

443:L37–40
Tafalla M, Bachiller R, Martín-Pintado J. 1993a. *Ap. J.* 403:175–86
Tafalla M, Bachiller R, Martín-Pintado J, Wright MCH. 1993b. *Ap. J. Lett.* 415:L139–42
Tafalla M, Bachiller R, Wright MCH. 1994. *Ap. J. Lett.* 425:L93–96
Tafalla M, Myers PC, Wilner DJ. 1995. In *Clouds, Cores, and Low Mass Stars*, ed. DP Clemens, R Barvainis, pp. 391–95. San Francisco: Astron. Soc. Pac. In press
Taylor S, Raga AC. 1995. *Astron. Astrophys.* 296:823–32
Taylor KNR, Storey JWV, Sandell G, Williams PM, Zealey WJ. 1984. *Nature* 311:236
Tenorio-Tagle G, Cantó J, Rózyczka M. 1988. *Astron. Astrophys.* 202:256–66
Terebey S. 1991. *Mem. Soc. Astron. Ital.* 62(4): 823–28
Terebey S, Chandler CJ, André P. 1993. *Ap. J.* 414:759–72
Terebey S, Vogel SN, Myers PC. 1989. *Ap. J.* 340:472–78
Torbett MV. 1984. *Ap. J.* 278:318–25
Torrelles JM, Ho PTP, Rodríguez LF, Cantó J, Moran JM. 1987. *Ap. J.* 321:884–87
Uchida Y, Shibata K. 1985. *Publ. Astron. Soc. Jpn.* 37:515–35
Umemoto T, Iwata T, Fukui Y, Mikami H, Yamamoto S, et al. 1992. *Ap. J. Lett.* 392:L83–86
van Dishoeck EF, Blake GA, Jansen DJ, Groesbeck TD. 1995. *Ap. J.* 447:760–82
Vogel SN, Kuhi LV. 1981. *Ap. J.* 245:960–76
Walker CK, Lada CJ, Young ET, Maloney PR, Wilking BA. 1986. *Ap. J. Lett.* 309:L47–51
Walker CK, Lada CJ, Young ET, Margulis M. 1988. *Ap. J.* 332:335–45
Walker CK, Narayanan G, Boss A. 1994. *Ap. J.* 431:767–82
Walmsley CM, Hermsen W, Henkel C, Mauersberger R, Wilson TL. 1987. *Astron. Astrophys.* 172:311–15
Walter FM, Brown A, Mathieu RD, Myers PC, Vrba FJ. 1988. *Astron. J.* 96:297–325
Ward-Thompson D, Chini R, Krügel E, André P, Bontemps S. 1995. *MNRAS* 274:1219–24
Ward-Thompson D, Scott PF, Hills RE, André P. 1994. *MNRAS* 268:276–90
Wardle M, Königl A. 1993. *Ap. J.* 410:218–38
Weintraub DA, Masson CR, Zuckerman B. 1989. *Ap. J.* 320:336–43
Welch WJW, Dreher JW, Jackson JM, Terebey S, Vogel SN. 1987. *Science* 238:1550–55
White GJ, Casali MM, Eiroa C. 1995. *Astron. Astrophys.* 298:594–605
Wilking BA, Mundy LG, Blackwell JH, Howe JE. 1989. *Ap. J.* 345:257–64
Wilner DJ, Welch WJ, Forster JR, Murata Y. 1995. Preprint
Wolf G, Lada CJ, Bally J. 1990. *Astron. J.* 100:1892–902
Wolfire MG, Königl A. 1993. *Ap. J.* 415:204–17
Yusef-Zadeh F, Cornwell TJ, Reipurth B, Roth M. 1990. *Ap. J. Lett.* 348:L61–64
Zhou S, Evans NJ II, Kömpe C, Walmsley CM. 1993. *Ap. J.* 404:232–46
Zhou S, Evans NJ II, Wang Y, Peng R, Lo KY. 1994. *Ap. J.* 433:131–48
Zinnecker H, Bastien P, Arcoragi JP, Yorke HW. 1992. *Astron. Astrophys.* 265:726–32
Zuckerman B, Kuiper TBH, Kuiper ENR. 1976. *Ap. J. Lett.* 209:L137–42